Int J Earth Sci (2000) 89 : 390–414

ORIGINAL PAPER

M.-P. Bolle · A. Pardo · K.-U. Hinrichs · T. Adatte
K. Von Salis · S. Burns · G. Keller · N. Muzylev

The Paleocene–Eocene transition in the marginal northeastern Tethys (Kazakhstan and Uzbekistan)

Received: 18 May 1999 / Accepted: 2 February 2000

Abstract We studied two sections that accumulated during the Paleocene–Eocene transition in shelf waters in the northeastern Tethys. Stable carbon isotopic compositions of marine and terrestrial biomarkers are consistent with a ^{13}C depletion in the oceanic and atmospheric carbon dioxide pools during the Late Paleocene Thermal Maximum (LPTM; Subzone P5b). The 2–3‰ negative $\delta^{13}C$ excursion in planktic foraminifera coincides with minimum $\delta^{18}O$ values, an incursion of transient subtropical planktic foraminiferal fauna, and the occurrence of an organic-rich sapropelite unit in Uzbekistan, which accumulated at the onset of a transgressive event. Biomarker distributions and hydrogen indices indicate that marine algae and bacteria were the major organic matter sources. During the Late Paleocene (Subzones P4 and P5a), the marginal northeastern Tethys experienced a temperate to warm climate with wet and arid seasons. Most likely, warm and humid climate initiated during the LPTM (Subzone P5b) and subsequently extended during the Eocene (Zone P6) onto adjacent land areas of the marginal northeastern Tethys.

Key words Northeastern Tethys · Late Paleocene · Thermal maximum · Climate · Clay minerals · Stable isotopes · Organic matter · Biomarkers

M.-P. Bolle (✉) · T. Adatte
Institut de Géologie, 11 Emile Argand, Université de Neuchâtel, CH-2007 Neuchâtel, Switzerland
e-mail: marie-pierre.bolle@geol.unine.ch
Tel.: +41-32-7182613
Fax: +41-32-7182601

A. Pardo
Departamento de Ciencas de la Tierre, Universidad de Zaragoza, E-50009 Zaragoza, Spain

K.-U. Hinrichs
Woods Hole Oceanographic Institution, Woods Hole, Massachusetts 02543, USA

K. von Salis
Geologisches Institut, ETH-Zentrum, CH-8092 Zürich, Switzerland

S. Burns
Geologisches Institut, Balzerstrasse, Universität Bern, CH-3000 Bern, Switzerland

G. Keller
Department of Geosciences, Princeton University, Princeton, New Jersey 08544, USA

N. Muzylev
Geological Institute, Russian Academy of Sciences, Pyzhevskii per.7, Moscow, 109017 Russia

Introduction

The Late Paleocene (~ 55.5 Ma) corresponds to one of the more prominent climatic changes in Earth history with a warming of 6–8 °C in deep and high-latitude surface waters (referred as Late Paleocene Thermal Maximum, or LPTM) (Kennett and Stott 1991; Zachos et al. 1993). Low-latitude surface temperatures remained relatively unchanged (Bralower et al. 1995; Thomas and Shackleton 1996). Sub-tropical to temperate faunas and floras in subpolar regions of both hemispheres (Estes and Hutchison 1980; Wolfe 1980; Axelrod 1984) coincide with warm (surface) water pelagic marine organism (Premoli-Silva and Boersma 1984; Kennett and Stott 1990; Lu and Keller 1993; Lu et al. 1998b; Pardo et al. 1999a, 1999b).

In both high and low latitudes, the warm pulse coincides with a pronounced short-term negative $\delta^{13}C$ excursion, which could have been caused by the release of methane hydrates during the LPTM (Sloan et al. 1992; Dickens et al. 1995, 1997). The $\delta^{13}C$ excursion is also associated with the extinction of 35–50 % of deep-sea benthic foraminiferal species (Thomas 1990; Kennett and Stott 1991), the radiation and proliferation of planktic foraminifera (Lu and Keller 1993, 1995; Pardo et al. 1999a, 1999b), and terrestrial vertebrates and plants (Gingerich 1980; Axelrod 1984).

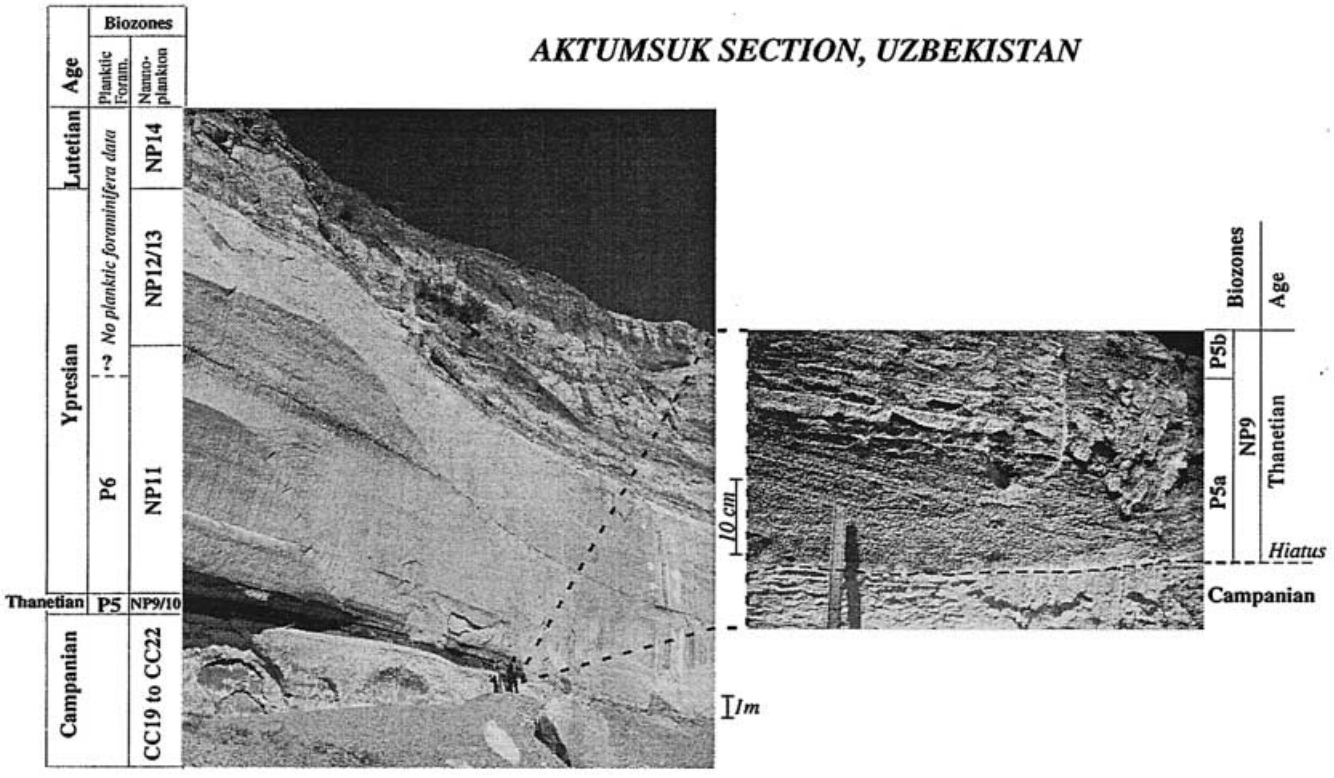

Fig. 1 The Aktumsuk section in Uzbekistan with a close-up on the P5a/P5b interval

Fig. 2 Panoramic view of the P/E transition at Kaurtakapy in Kazakhstan

Clay mineral compositions of oceanic sediments indicate a time of high rainfall with enhanced chemical weathering in Antarctic, South Atlantic (Robert and Chamley 1991; Robert and Kennett 1992, 1994), and North Atlantic oceans (Knox 1996; Gibson et al. 1993; Gawenda et al. 1999). In contrast, the southern margin of the Tethys region (Saharan Platform and Arabian Peninsula) is characterized by increased aridity and enhanced evaporation as indicated by the occurrence of palygorskite and sepiolite and the presence of evaporites (Mélières 1977; Robert 1982; Oberhänsli 1992; Bolle et al. 1999).

During the Late Paleocene, the marginal northeastern Tethys was characterized by the accumulation of an organic-rich layer called "sapropelite unit", which is correlatable over vast areas in Central and South Asia, Caspian Region, and Caucasus (Gavrilov and Muzylev 1991; Muzylev et al. 1994; Gavrilov et al. 1997).

This study evaluates the Paleocene–Eocene (P–E) transition in Uzbekistan and Kazakhstan based on two sections, Aktumsuk and Kaurtakapy (Figs. 1, 2), and consists of an integrated multidisciplinary approach that includes micropaleontology, sedimentology, mineralogy, and geochemistry. Due to their particular paleogeographic location, these sections provide an important new data set which is crucial for a better understanding of the climatic and environmental changes across the P–E transition, in the shallow northern marginal seas of the Tethys.

Location and paleogeographic setting

The Kaurtakapy section is located in the Kazakhstan desert, approximately 60 km from the Caspian Sea at 44°15′N and 52°19′E. The Aktumsuk section is located near the Aral Sea in Uzbekistan at 43°85′N and 57°17′E (Fig. 3). Paleogeographic reconstructions for the Paleocene (Thanetian-Danian) and Early Eocene (Ypresian; Smith et al. 1994) reveal several

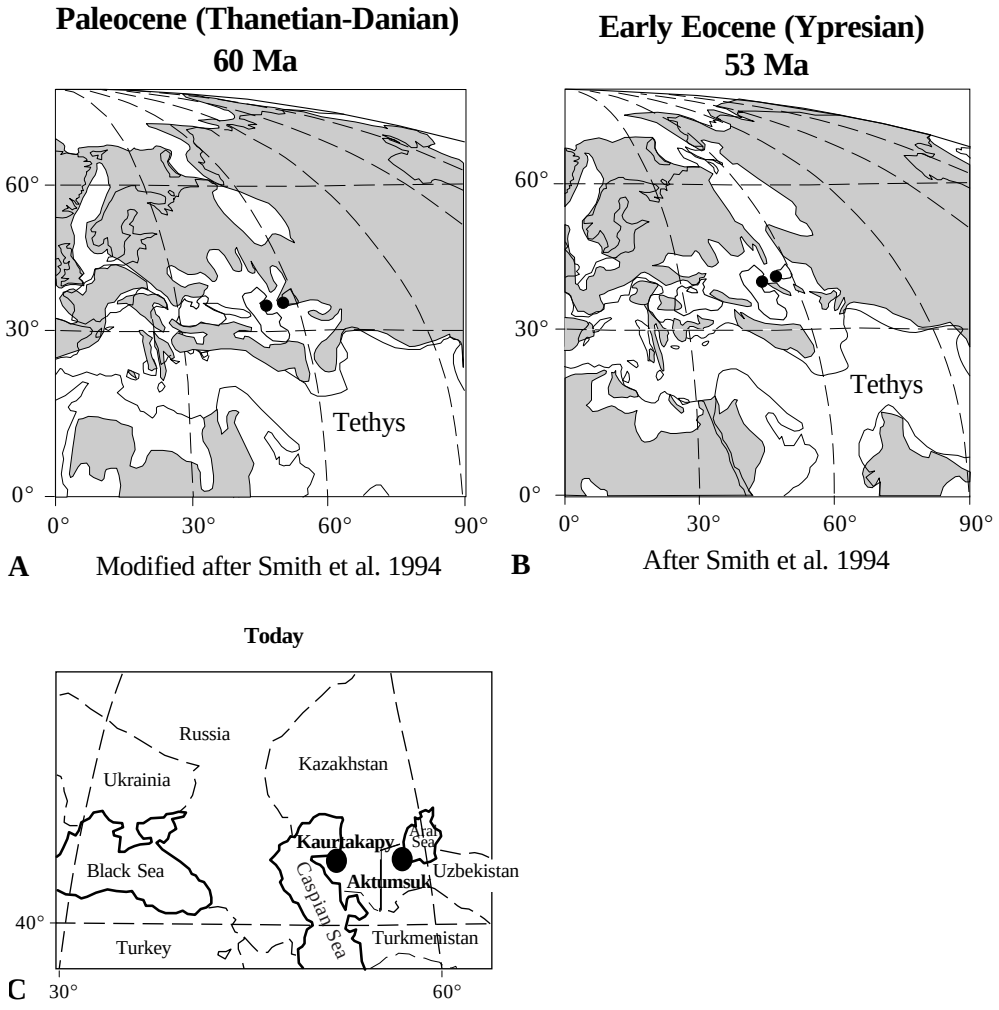

Fig. 3 **A** Inferred paleogeographic map during the Paleocene at 60 Ma (Thanetian–Danian). **B** Inferred paleogeographic map during the Early Eocene at 53 Ma (Ypresian) **C** Geographical location of the Aktumsuk (Uzbekistan) and Kaurtakapy (Kazakhstan) sections

global tectonic events that may have affected climate and oceanic circulation (Fig. 3). During most of the Paleocene, the sediments of the Kaurtakapy section were deposited in a restricted shallow area in the marginal northern part of the Tethys connected to the open sea by two narrow gateways trending north–south and east through the Crimean Sea. At Aktumsuk the presence of a major hiatus (see Discussion) suggests a location close to an emerged continental area during the Paleocene (Fig. 3). During the Early Eocene this part of the NE Tethys was marked by two major events: (a) the opening of an important connection with the Arctic Ocean to the north; and (b) a reduction of emerged lands to the southeast. During this period, increased oceanic circulation and oxygenation of the bottom waters characterized the marginal northeastern Tethys.

Lithology

Kaurtakapy

We studied a 27 m thick sequence that spans the planktic foraminiferal zones P4–P6b (Fig. 4). The Sulukapy formation (Kusnetsova 1952) consists of 10 m of sandy chalks, overlain by 3 m of sandy marls and 1 m of marls. The sandy marls contain sea urchins, phosphorite pebbles, and burrowings. The base of the Givmra formation (Kusnetsova 1952) is marked by 10 cm of brown clays containing fish scales and pyrite nodules partly oxidized in goethite. This clay layer is overlain by 10 m of grayish to reddish marls. Although no hard-ground surface has been observed, the sharp contact between these two formations suggests a break in sedimentation. The uppermost 2 m of reddish chalks correspond to the Tschat Formation (Kusnetsova 1952). The Paleocene and Eocene parts were collected in two outcrops approximately 5 km apart. In the first outcrop, the Sulukapy Formation, is exposed up to the base of the Eocene and includes the 10 cm thick clay layer. In the second outcrop, the

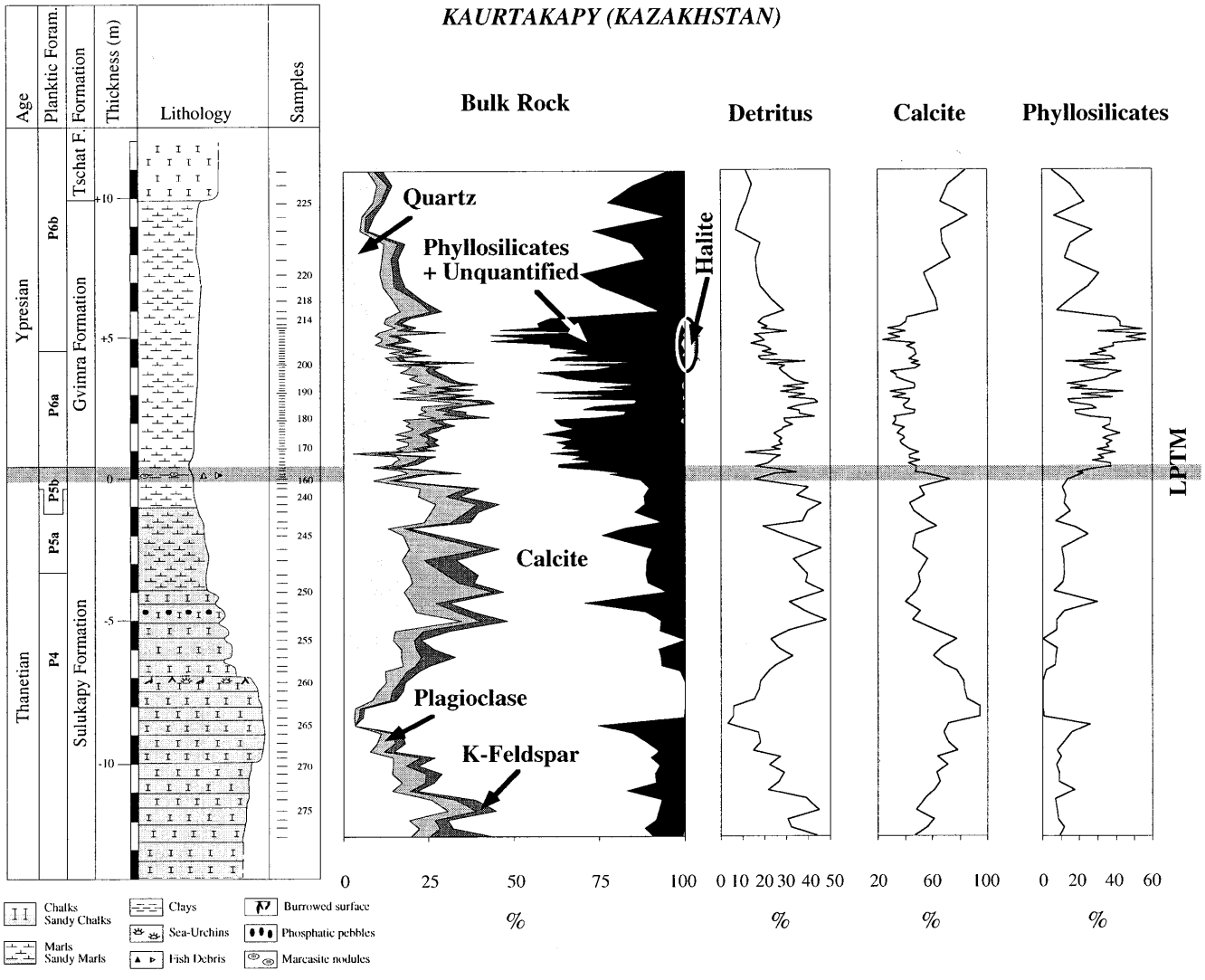

Fig. 4 Lithologic log with sample locations and bulk-rock mineral composition at Kaurtakapy (Kazakhstan). Detritus includes quartz, potassic feldspar, and plagioclase. Planktic foraminiferal biozonation used in this study are from Berggren et al. (1995) modified by Pardo et al. (1999a, 1999b). Formations used in the log are from Kusnetsova (1952). The shaded layer corresponds to the Late Paleocene Thermal Maximum (LPTM) interval

section begins 1.5 m below the clay layer and continues into the lower Eocene (Givmra Formation). Samples were collected below and above the brown clay interval used to correlate the two sections.

Aktumsuk

Aktumsuk is 32 m thick and spans nannofossil zones CC 19 to NP14 (Fig. 1). Although this report focuses on the 6 m interval spanning the late Paleocene to early Eocene nannofossil zones NP9–NP11 and planktic foraminiferal Subzone P5a to Zone P6 (Figs. 5). A major hiatus and strong bioturbation mark the base of this interval. At this unconformity Campanian white chalks containing sea urchins, belemnites, and oyster shells are overlain by late Paleocene (P5a) sediments. The P5a interval is a 20 cm thick gray chalk with low organic matter content, phosphatic pebbles, and cross bedding. The P5b interval is ~1 m thick and can be divided in two parts: (a) a 50 cm thick dark-gray cross-bedded chalk with wood fragments; and (b) a 50 cm thick gray chalk with parallel stratification which is bioturbated in the uppermost 20 cm. The upper part of the section (Zone P6) consists of two white massive chalks beds separated by a thin clay layer of 10 cm.

Ilyin and Boiko (1989) indicate the presence of reworked and resedimented phosphorite pebbles in lower Paleocene sediments of the western part of Uzbekistan near the Aral Sea. At Aktumsuk, phosphorite nodules are found in Zone P5a above the unconformity and erosion surface where the lower part of the Paleocene and the whole Maastrichtian is missing.

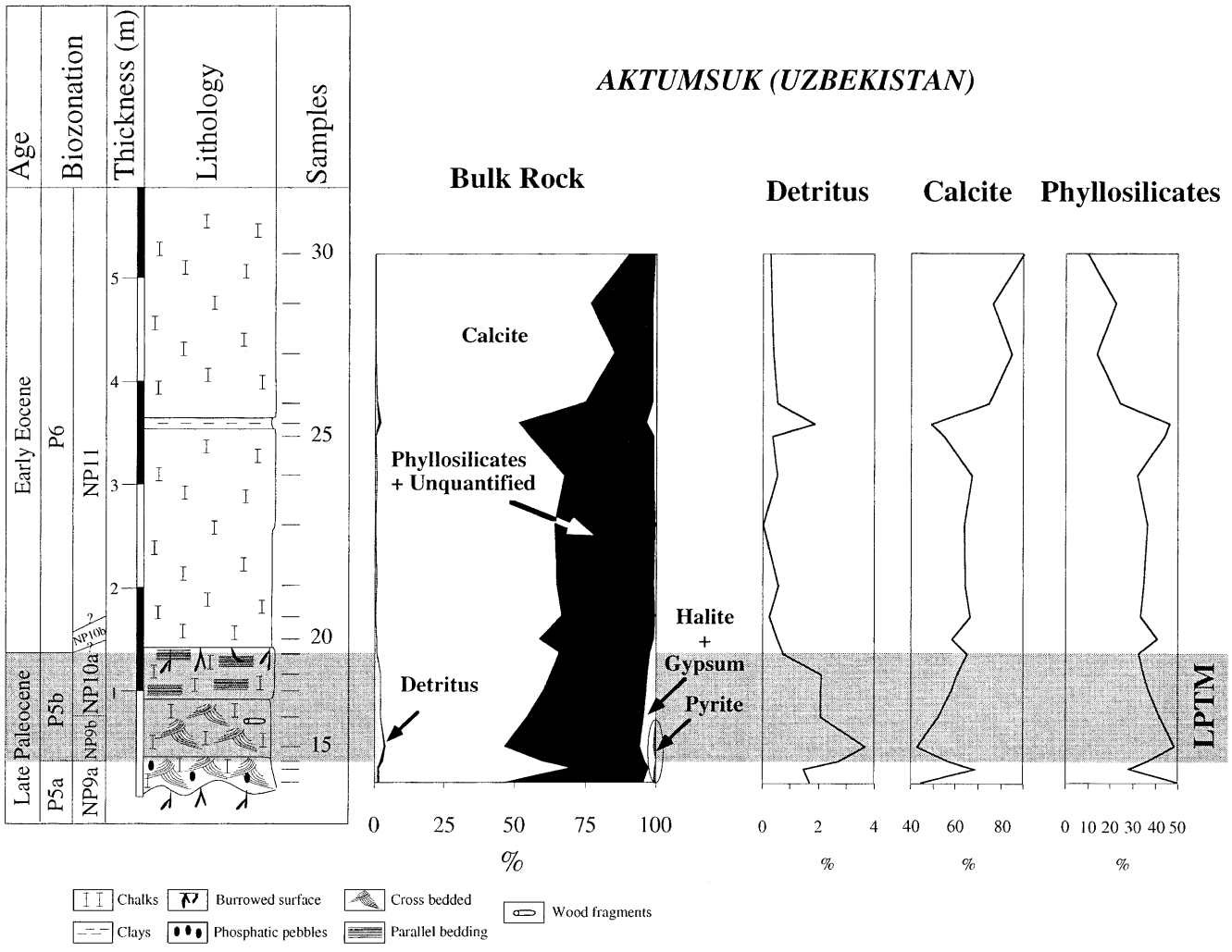

Fig. 5 Lithologic log with sample locations and bulk-rock mineral composition at Aktumsuk (Uzbekistan). Detritus includes quartz and plagioclase. Planktic foraminiferal and nannofossil biozonations used in this study are from Berggren et al. (1995) modified by Pardo et al. (1999a, 1999b) and Martini (1971). The shaded layer corresponds to the LPTM interval

Methods

The sections were measured and samples were collected from all lithological units. A total of 100 samples were collected from the Kaurtakapy and 30 samples from the 6 m interval of the Aktumsuk sections, respectively. Identification and biostratigraphic determinations of planktic foraminifera were carried out on the size fraction greater than 106 μm. Scanning electron microscopic photomicrographs of planktic foraminiferal specimens were taken at the University of Neuchâtel (Switzerland). Sixteen samples were chosen and prepared for the study of calcareous nannofossils of the Aktumsuk section. Simple smearslides were studied with a light microscope at a 1000× magnification.

X-ray diffraction (XRD) analyses of whole rock and clay mineral studies were conducted at the Geological Institute of the University of Neuchâtel, using a SCINTAG XRD 2000 diffractometer with standard errors varying between 5 and 10 % for the phyllosilicates and <5 % for grain minerals. Whole-rock samples were prepared following the procedure of Kübler (1987). For each rock sample, approximately 20 g were ground to obtain small rock chips (1–5 mm); of these, 5 g were dried at a temperature of 60 °C and then ground again to a homogenous powder with particle sizes <40 μm. Eight hundred milligrams of this powder were compressed (20 bars) in a powder holder and analyzed by XRD. Whole-rock compositions were determined using external standards based on methods described by J. Ferrero (unpublished data), Kübler (1983), and Moore and Reynolds (1989).

Clay mineral analyses were based on the methods by Kübler (1987). The carbonate fraction of ground chips was removed with 10 % of HCl (1.25 N) at room temperature for 20 min or more until all the carbonate was dissolved. The insoluble residue was washed and centrifuged until a neutral suspension was obtained

(pH 7–8). Different grain-size fractions (< 2 μm and 2–16 μm) were obtained by the timed settling method based on Stokes Law and pipetted onto a glass plate. The intensities of selected XRD peaks characterizing each clay mineral were measured for a semi-quantitative estimate of the proportion of clay minerals present in the two size fractions (< 2 μm and 2–16 μm); therefore, clay minerals are given in percent abundance and in counts per minute without correction factors. The clay mineral ratios are calculated from XRD mineral peak data in counts per minute.

Rock Eval analysis was performed with a Rock Eval 6 pyrolyser at the Geological Institute of the University of Neuchâtel, following the analytical methods of Espitalié et al. (1985, 1986) and Lafargue et al. (1996). Among other parameters, this technique allows the determination of the total organic carbon (TOC) content and the hydrogen index (HI, mg HC/g TOC). The latter parameter was calculated from TOC data and the absolute amount of hydrocarbons generated during kerogen pyrolysis (S2 peak), and is commonly used to characterize the organic matter quality. The temperature of maximum hydrocarbon generation during temperature-programmed pyrolysis (T_{max}) can be used to characterize the maturity of the organic material.

Analyses of lipid biomarkers, undertaken with organic carbon-rich samples from Aktumsuk, are described by Hinrichs et al. (1999a). Briefly, free lipids were extracted using a Dionex Accelerated Solvent Extraction 200 system at 100 °C and 1000 psi with dichloromethane/methanol (99 : 1 v/v) as the solvent. Extracts were separated in four fractions of increasing polarity (hydrocarbons, ketones/esters, alcohols, and carboxylic acids) using SUPELCO LC-NH2 glass cartridges by applying a sequence of solvent mixtures of increasing polarity. Individual compounds were quantified and identified using a HP 6890 GC equipped with a J&W DB-5 (60 m length, 0.32 mm inner diameter, and 0.25 μm film thickness) capillary column and coupled to a HP 5973 MSD. Stable carbon isotopic compositions of individual compounds were determined using a Finnigan Delta Plus isotope mass spectrometer coupled to a HP 6890 GC and equipped with a column identical to that described above. Hydroxyl- and carboxyl derivatives were analyzed as their trimethylsilyl ethers or esters, respectively, after reaction with BSTFA. Reported δ values are corrected for the introduction of additional carbon atoms by derivatization. Bacteriohopanepolyol was cleaved according to procedures described by Rohmer et al. (1984), and the resulting hopanols were analyzed as acetates. Carbon isotopic compositions of total organic carbon at Aktumsuk were determined by combustion (sealed quartz tube, CUO/Ag, 850°, 8 h) and isotopic mass spectrometry (Micromass Optima) after dissolution of carbonates, using a ~30 % (H_3PO_4) and subsequent removal of excess water by vacuum treatment.

Stable isotopic analyses were performed on the fine fraction (< 63 μm) of Aktumsuk samples, which is composed mainly of foraminifera, nannoplankton, and detrital particles such as quartz. Additionally, we performed analyses on mixed assemblages of planktic foraminifera. For each sample approximately 70 specimens in the size fraction of 125–250 μm were selected. Analyses of the fine fraction and the foraminifera were conducted at the Stable Isotope Laboratory of the University of Bern (Switzerland) using a VG Prism II ratio mass spectrometer equipped with a common acid bath (H_3PO_4). The results were calibrated to the PDB scale with standard errors of 0.1‰ for $\delta^{18}O$ and 0.05‰ for $\delta^{13}C$.

Biostratigraphy

Aktumsuk

Planktic foraminifera

Planktic foraminiferal biostratigraphy of the Aktumsuk section is based on the zonation by Berggren et al. (1995), though Zone P5 has been subdivided into Subzones P5a and P5b based on the first appearance datum of *Acarinina sibaiyaensis* and/or *A. africana* (Fig. 6; Pardo et al. 1999a). Preservation of planktic foraminifera is very good and surface textures and most morphological features are easily identifiable, although calcite tests are sometimes recrystallized (Figs. 7, 8).

The base of the Aktumsuk section is characterized by a major hiatus that juxtaposes Campanian and late Paleocene (P5a) sediments (uppermost Thanetian). The P–E transition appears to be relatively complete, although some biozonal markers (e.g., *Morozovella formosa*) are absent in the assemblage.

Zone P5 is defined by the last appearance (LA) of *Luterbacheria (Globanomalina) pseudomenardii* at the base and the LA of *Morozovella velascoensis* at the top, and the duration of this biozone is estimated from 55.9 to 54.7 Ma (Berggren et al. 1995). Zone P5 is subdivided into two subzones based on the first appearance (FA) of *A. sibaiyaensis* and/or *A. africana*. The FA of these two short-ranging taxa coincides in the Tethys with the benthic foraminiferal extinction event (BFEE), the negative carbon shift, and the planktic foraminiferal diversification that characterize the P–E climatic event (Pardo et al. 1999a). Characteristic assemblages of Zone P5 include *M. velascoensis*, *M. subbotinae*, *Subbotina velascoensis*, *S. eocaenica*, *Igorina pusilla*, *I. convexa*, *I. reissi*, *Acarinina acarinata*, *A. sibaiyaensis*, and *A. strabocella*.

Subzone P5a is defined by the biostratigraphic interval between the LA of *L. pseudomenardii* at the base and the FA of *A. sibaiyaensis* and/or *A. africana* at the top (Fig. 6). The age of Subzone P5a is from 55.9 to 54.8 Ma (1.1 m.y. duration, assuming that the

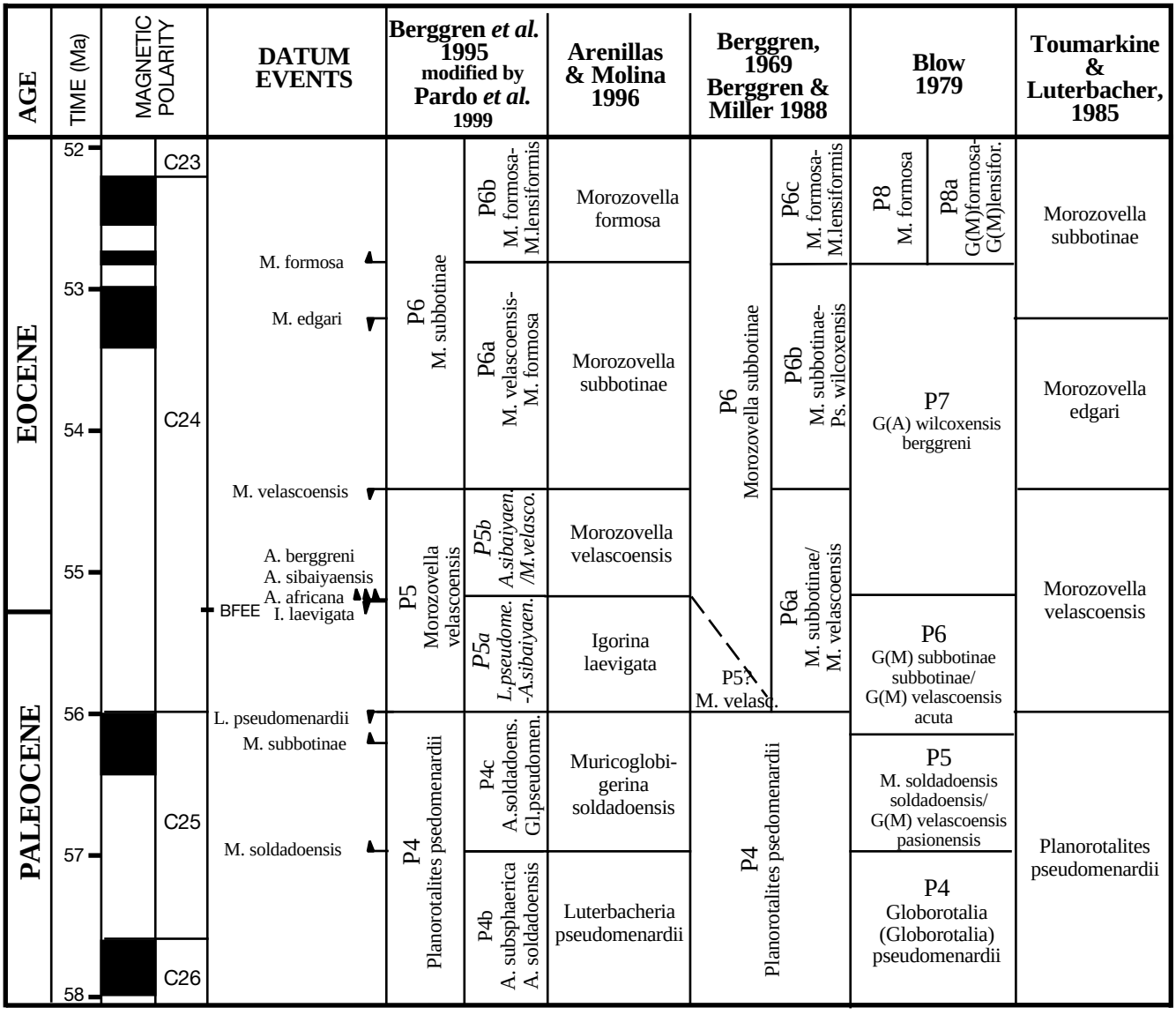

Fig. 6 Planktic foraminiferal zonations across the Paleocene–Eocene transition with the datum events used at Aktumsuk in comparison with other commonly used zonal schemes for the Paleogene (Berggren 1969; Blow 1979; Toumarkine and Luterbacher 1985; Berggren and Miller 1988; Berggren et al. 1995; Arenillas and Molina 1996; Pardo et al. 1999a). Magnetostratigraphic and absolute age chronologic schemes and their correlation with planktic foraminiferal datum events are based on Cande and Kent (1992) and Berggren et al. (1995). BFEE benthic foraminiferal extinction event

FA of *A. sibaiyaensis* and/or *A. africana* is coincident with the BFEE and the $\delta^{13}C$ excursion; Berggren et al. 1995). At Aktumsuk, Subzone P5a spans from sample 12 to sample 15 (~ 32 cm) and the sediment accumulation rate is estimated at 0.3 mm/1000 years. This very low sedimentation rate could be an artifact due to the hiatus observed at the base of Subzone P5a (Fig. 5).

Subzone P5b is defined by the FA of *A. sibaiyaensis* and/or *A. africana* at the base and the LA of *M. velascoensis* at the top (Fig. 6). The estimated age range is from 54.8 to 54.7 Ma (0.1 m.y. duration; Berggren et al. 1995). At Aktumsuk, Subzone P5b has been identified by the occurrence of *A. sibaiyaensis* and spans from sample 15 to sample 20 (~ 88 cm; sediment accumulation rate of 8.8 mm/1000 years). In this section minimum $\delta^{13}C$ and $\delta^{18}O$ values, along with an increase in transient subtropical planktic foraminiferal fauna characterize Subzone P5a. This subtropical incursion is characterized by maximum igorinid abundance in sample 18 (Pardo et al. 1999b).

Zone P6 is defined by the LA of *M. velascoensis* at the base and the FA of *M. aragonensis* at the top and spans from 54.7 to 52.3 Ma (Berggren et al. 1995). This zone is divided into two subzones. Subzone P6a is defined by the LA of *M. velascoensis* at the base and the FA of *M. formosa* at the top, and spans from 54.7

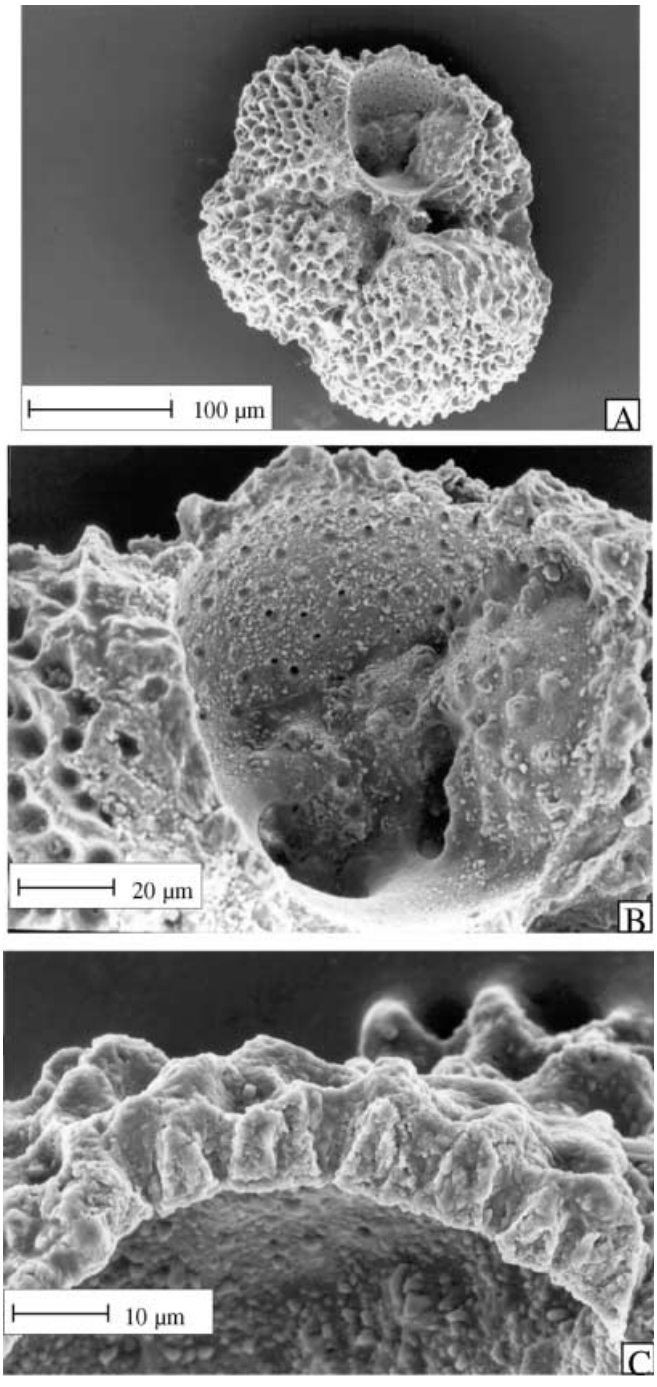

Fig. 7A–C Scanning electron microscope photomicrographs of *Acarinina soldadoensis* (Aktumsuk; sample AM13). **A** External view; **B** Fractured chamber lack infillings; **C** small pores that traverse test wall lack infillings

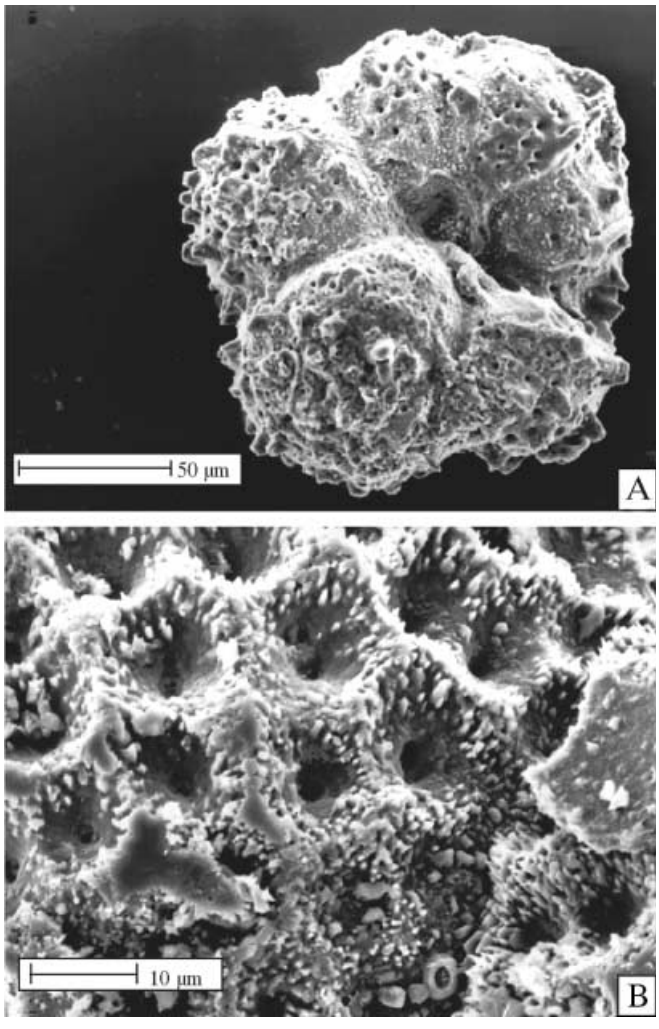

Fig. 8A,B Scanning electron microscope photomicrographs of *Acarinina* cf. *sibaiyaensis* (Aktumsuk; sample AM18). **A** External view of the specimen. Note the partial dissolution of the test. **B** Calcite overgrowth around small pores

to 54.0 (Berggren et al. 1995). Subzone P6b is defined by the FA of *M. formosa* at the base and the FA of *M. aragonensis* at the top, with an estimated age range from 54.0 to 52.3 Ma (Berggren et al. 1995). At Aktumsuk, the P6a/P6b boundary was not identified due to the absence of the index species *M. formosa*.

Calcareous nannofossils

Species concepts used are mainly those of Perch-Nielsen (1985), and the standard zonation of Martini (1971) is used with the additional subdivision of Aubry (1996).

The Paleogene section studied lies on Late Campanian sediments characterized by well-preserved calcareous nannofossils (e.g., *Eiffellithus eximius*, *Reinhardtites anthorphorus*, *Aspidolithus parcus*, and *Arkhangelskiella cymbiformis*).

The lowermost Paleogene sample (sample 12) contains well-developed assemblage of Late Paleocene calcareous nannofossils. The presence of *Discoaster multiradiatus* and *Fasciculithus tympaniforis* without *Campylosphaera eodela* or any *Rhomboaster* species suggests Zone NP9a of Martini (1971). Samples 14 and 15 include *C. eodela* and can be assigned to Zone

NP9b. Both discoasters and fasciculiths are rare in these assemblages.

The base of Zone NP10a is defined by the FA of *Rhomboaster bramlettei* and was found in sample 16, where very rare *R. bramlettei* are accompanied by *Discoaster anartios* and very rare fasciculiths. Sample 20 contains *Discoaster* cf. *D. mahmoudii* and possibly *Tribrachiatus digitalis* and large *Lophodolithus* sp., suggesting Zone NP10b as defined by Aubry (1996). The remaining samples do not include markers for the following zones and thus may be assigned to NP11, which is defined by the LA of *Tribrachiatus contortus* at the base and the FA of *Discoaster lodoensis* at the top (Fig. 5); however, the two markers of NP11 were not found in the samples. This assignment is also supported by the absence of *D. lodoensis* in higher samples than those shown here. The absence of *T. contortus* and *D. lodoensis* may be due to the relatively shallow water depth of the Aktumsuk section.

Frequent specimens of the genus *Transversopontis* and *Pontosphaera* and rare *Braarudosphaera bigelowii* were found in most Paleogene samples. All these forms indicate usually relatively shallow-water conditions.

All samples contain rarely to moderately reworked Upper Cretaceous – mainly Campanian – calcareous nannofossils (*Eiffellithus eximius*, *Reinhardtites anthorphorus*, *Aspidolithus parcus, Quadrum trifidum, Micula decussata, Watznaueria barnesae, Gartnerago obliquum*, and many other species).

Kaurtakapy

Planktic foraminifera

The biostratigraphy of the Kaurtakapy section is detailed by Pardo et al. (1999a); however, some events are mentioned to facilitate the comparison and correlation with the Aktumsuk section.

Zone P4 defined by the total range of *Luterbacheria* (*Globanomalina*) *pseudomenardii* (Berggren et al. 1995) has been identified in the Kaurtakapy section (Fig. 4). This zone has a thickness of 860 cm and an estimated average sediment accumulation rate of 3.9 mm/1000 years, although the base may not have been recovered.

Subzone P5a spans 310 cm and the sediment accumulation is estimated at 2.8 mm/1000 years. This low sedimentation rate could be due to condensed sedimentation and/or a hiatus at the lithological change from marls to clay at the LPTM interval (Fig. 4).

Subzone P5b spans only 40 cm including the clay layer (sediment accumulation rate 0.8 mm/1000 years), suggesting again a condensed interval and/or the presence of a hiatus as noted by the sharp lithological contact between the clay layer and the overlaying marls. The $\delta^{13}C$ excursion and the rapid planktic foraminiferal diversification occur within this subzone (Fig. 9).

At Kaurtakapy the P6a/P6b boundary was identified due to the presence of the index species *M. formosa*. Subzone P6a spans 470 cm and the average sediment accumulation rate is estimated at 7 mm/1000 years, whereas Subzone P6b spans 520 cm and the top was not recovered.

Mineralogy

Bulk rock

Kaurtakapy

Whole-rock analyses show that the dominant component of the sediments is calcite (Fig. 4). From the base to −8 m calcite content increases from 45 to 90 %. Between −8 and 0 m calcite gradually decreases to an average value of 52 %. The onset of the LPTM is marked by a decrease in calcite from 75 to 50 %. Relatively low calcite content persists in the first 5 m of the Gvimra Formation reaching a minimum value of 22 %. The last 7 m of section, including the top of the Gvimra and the base of the Tschat formations, are marked by increased calcite content of up to 65 % (Fig. 4). In the Sulukapy Formation (first 12 m) calcite variations coincide mainly with changes in quartz, plagioclase, and potassic feldspar, whereas in the lowermost 5 m of the Gvimra Formation decreased calcite corresponds with increased phyllosilicates from 30 to 49 %. In this section quartz, plagioclase, and potassic feldspar constitute an important component of the sediments with an average of 26 % and a maximum of 49 %.

Aktumsuk

The sediment is dominated by calcite and phyllosilicates with minor components of quartz and plagioclase, evaporite minerals (halite and gypsum), and some pyrite (Fig. 5). Gypsum is present in veins into the sediments, whereas the proximity of the Aral Sea may explain the presence of halite in traces in the section. From P5a to P6 calcite gradually increased from 45 to 85 %, whereas phyllosilicates decreased from 40 to 15 % except within a clay layer (sample 26), where quartz and phyllosilicates exhibited higher values, 2 % and 48 %, respectively. In this section the P5b interval is marked by relatively high quartz (~3 %) and low calcite (~42 %) contents and the presence of pyrite (Fig. 5).

The main mineralogical difference between the two sections is the higher detritus content at Kaurtakapy (26 %) as compared with Aktumsuk (1 %), and the dominance of calcite at Aktumsuk vs phyllosilicates and detrital minerals at Kaurtakapy.

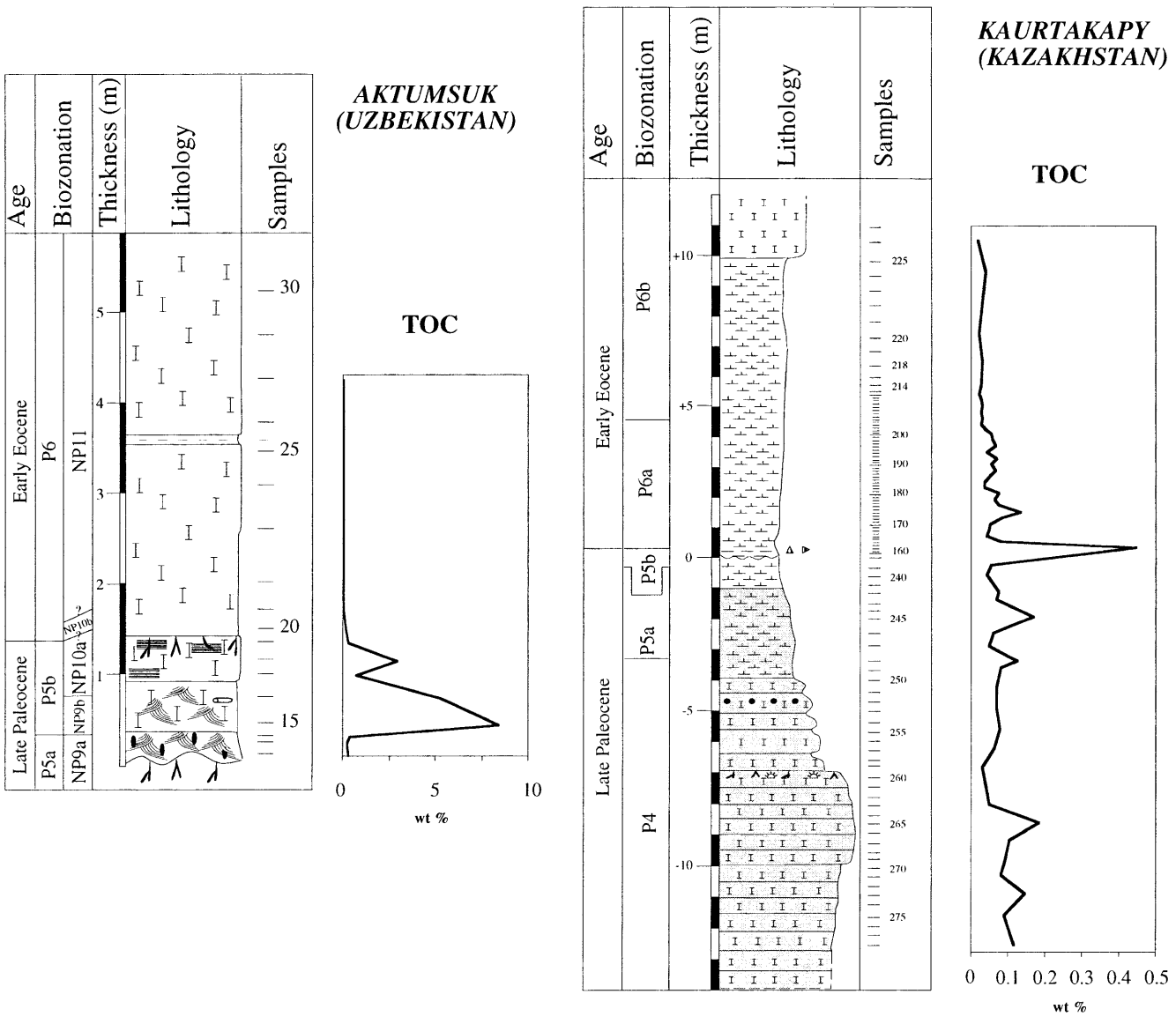

Fig. 9 Total organic carbon (TOC) at Aktumsuk (Uzbekistan) and Kaurtakapy (Kazakhstan). See Figs. 2 and 3 for symbol explanation

Clay mineralogy

Kaurtakapy

Smectite, with an average of 55 %, dominates the clay fraction in the lower 20 m (Zones P4–P6a) and decreases to 0 % in P6b. This decrease coincides with increased mica and chlorite contents up to 65 and 20 %, respectively. Kaolinite is sporadically present in the first 15 m of the section (P4–P5b), increases gradually in P6a (2 %), and reaches a maximum of 10 % in Zone P6b (Fig. 10). Mixed-layers illite–smectite (IS) are minor components of the clay fraction (3 %). The onset of the LPTM is marked by an increase in kaolinite from 0.5 to 3 %, mica from 14 to 30 %, and by an important decrease in smectite from 77 to 54 %.

Aktumsuk

Smectite, mica, and kaolinite dominate the clay fraction. Chlorite (9 %) and IS (8 %) are minor components throughout the section (Fig. 11). From the base of the section to the clay layer (sample 26), smectite and mica with an average value of 27 and 29 %, respectively, show only minor variations in their con-

Fig. 10 Clay mineral composition and kaolinite/smectite ratio at Kaurtakapy (Kazakhstan). Clay minerals are given in relative percent abundance and the clay mineral ratio is calculated from XRD mineral peak data in counts per minute. See Fig. 4 for symbol explanation

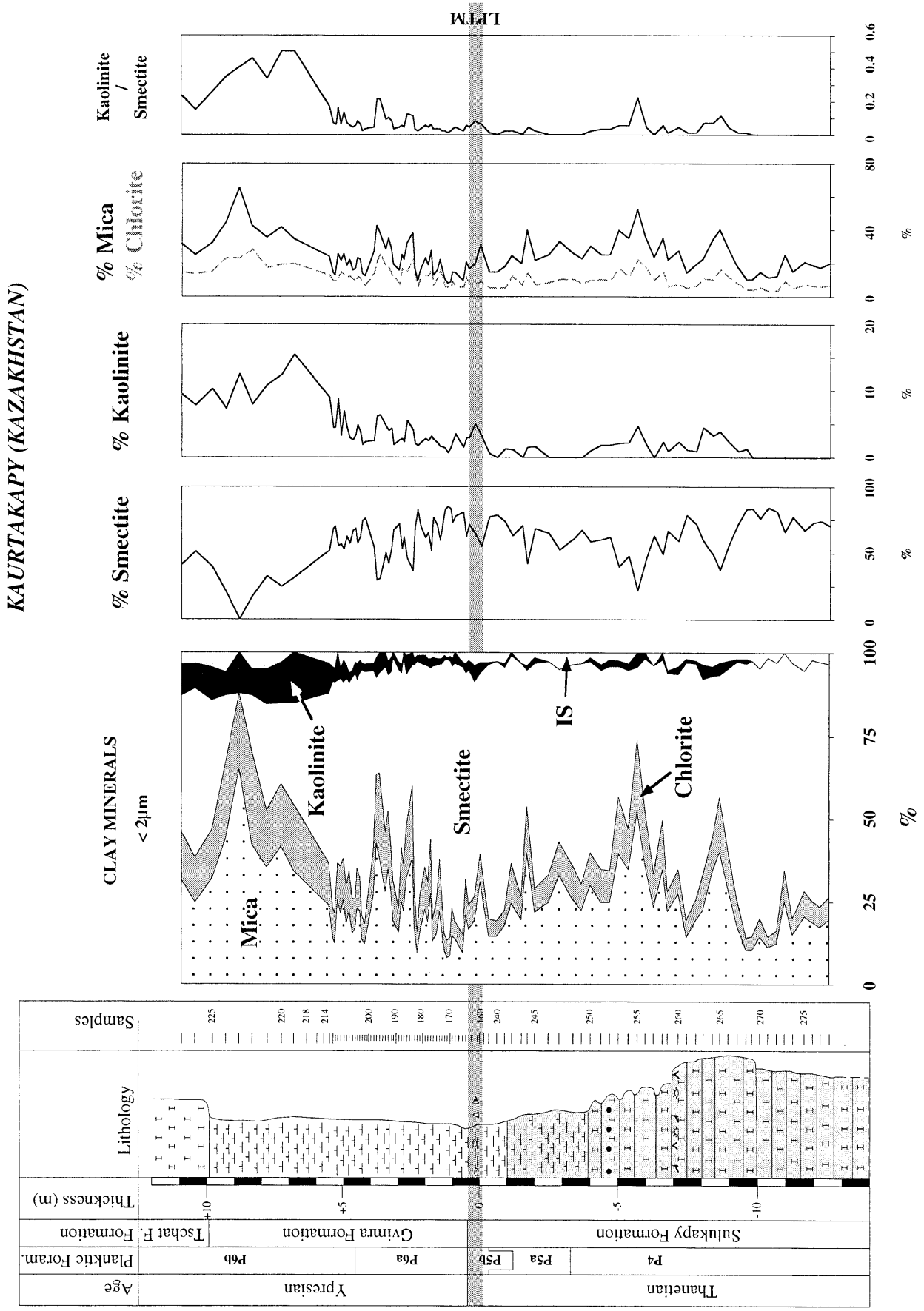
KAURTAKAPY (KAZAKHSTAN)
CLAY MINERALS
< 2µm
Mica
Kaolinite
Smectite
IS
Chlorite
%
% Smectite
% Kaolinite
% Mica
% Chlorite
Kaolinite / Smectite
LPTM
Samples
Lithology
Thickness (m)
Age
Planktic Foram.
Tschat F. Formation
Gyimra Formation
Sulukapy Formation
Thanetian
Ypresian
P4
P5a
P5b
P6a
P6b

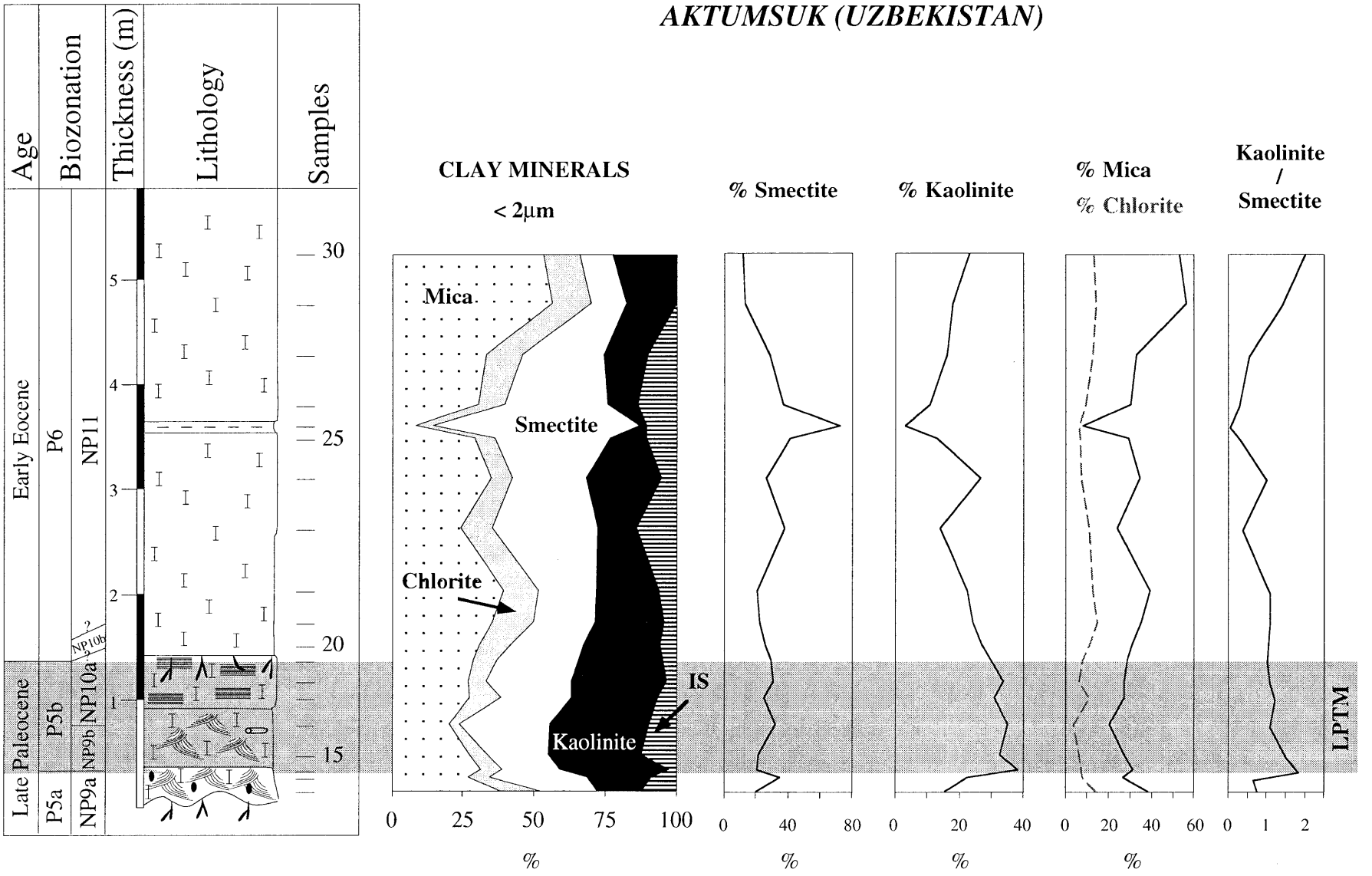
AKTUMSUK (UZBEKISTAN)
Age
Biozonation
Thickness (m)
Lithology
Samples
Early Eocene
Late Paleocene
P6
P5b
P5a
NP11
NP10b
NP10a
NP9b
NP9a
CLAY MINERALS
< 2µm
Mica
Smectite
Chlorite
Kaolinite
IS
% Smectite
% Kaolinite
% Mica
% Chlorite
Kaolinite / Smectite
LPTM
0 25 50 75 100
%
0 40 80
0 20 40
0 20 40 60
0 1 2
30
25
20
15
5
4
3
2
1

Fig. 11 Clay mineral composition and kaolinite/smectite ratio at Aktumsuk (Uzbekistan). Clay minerals are given in relative percent abundance and the clay mineral ratio is calculated from XRD mineral peak data in counts per minute. See Fig. 5 for symbol explanation

tent. From P5a to P5b kaolinite increases from 22 to 37 %. A high kaolinite content persists during the P–E event, and then decreases to reach a minimum value in the clay layer (3 %).

The clay layer in Zone P6 (sample 26) is marked by a strong increase in smectite (72 %) and relatively low mica (8 %) and kaolinite (3 %) contents. From the clay layer to the top of the section, mica and kaolinite increase gradually to reach a maximum of 53 % and 20 %, respectively, whereas smectite decreases to 11 %.

During the P–E event the main difference observed between the two sections is the higher kaolinite content at Aktumsuk (32 %) as compared with Kaurtakapy (2 %).

Stable isotopes

Fine fraction

$\delta^{13}C$ values of the fine fraction (< 63 μm) decrease abruptly from 1.6 to 0.17‰ reaching a minimum value of −0.66‰ in the P5b interval (Fig. 12; Table 1). The post-$\delta^{13}C$ shift recovers gradually from −0.35to 1.7‰ with the exception of the sample 24 where the $\delta^{13}C$ value is near zero. $\delta^{18}O$ values of the fine fraction (< 63 μm) gradually decrease from −2.2 to −4.27‰ reaching a minimum value of −5.05‰ in the P5b interval (sample 18). The post-$\delta^{18}O$ recovery is also gradual, from −4.1 to −2.8‰, with the exception of sample 24 where the value decreases to −3.7‰.

Foraminifera

The $\delta^{13}C$ record of the mixed planktic foraminiferal assemblage shows a similar trend across the Paleocene–Eocene transition as observed for the fine fraction (Fig. 12). $\delta^{13}C$ values decrease abruptly from 1.4 to −0.19‰ reaching a minimum of −1.24‰ (sample 18; Fig. 12; Table 1). The post-$\delta^{13}C$ shift gradually recovers from −0.89 to 0.47‰. The $\delta^{18}O$ record also shows a similar trend to that of the fine fraction, with a gradual decrease from −2.28‰ to a minimum value of −4.95‰ (Fig. 12; Table 1). The post-$\delta^{18}O$ recovery is also gradual from −4.52 to −3.2‰.

At Kaurtakapy carbon and oxygen stable isotope analyses were carried out on specimens of benthic foraminifer *Cibicidoides* spp. (Pardo et al. 1999a). The $\delta^{13}C$ record from the Kaurtakapy section shows a gradual decrease from 2.56 to 1.35‰ during the Late Paleocene (Zones P4 and P5a) with a total decrease of 1.2‰ during the last 9 m up to the clay layer (Fig. 12). The main shift begins at the clay layer at 1.35‰ and reaches a minimum value of 0.25‰ 30 cm above the base of the clay layer. This carbon shift coincides with increased species richness and relative abundance of warm-water species (Pardo et al. 1999a). The post-$\delta^{13}C$ shift recovery is approximately 1.2‰, relatively rapid, and occurs within the 90 cm of marls above the clay layer (Fig. 12).

Table 1 Aktumsuk section. Stable isotopes ($\delta^{13}C$ and $\delta^{18}O$) values and total organic carbon (TOC; wt. %) with the hydrogen index (HI) and maximum temperature (T_{max}). See Fig. 5 for sample position

					Fine fraction (< 63 μm)		Mixed planktic foraminifera	
Sample	T_{max} (°)	HI	TOC (%)	$\delta^{13}C$ (TOC)	$\delta^{13}C$	$\delta^{18}O$	$\delta^{13}C$	$\delta^{18}O$
AM12	376	23	0.35		1.596	−2.202	0.58	−2.28
AM13	420	39	0.23	−24.30	1.68	−2.73	1.44	−3.12
AM14	434	303	0.38	−28.64	0.17	−3.37	1.14	−3.44
AM15	419	398	8.44	−30.35	−0.09	−3.67	−0.19	−4.02
AM16	426	416	5.27	−30.22	−0.25	−4.27	−0.72	−4.98
AM17	437	267	0.78	−28.84	−0.17	−4.08	−0.88	−4.58
AM18	428	357	2.94	−29.83	−0.66	−5.05	−1.24	−4.72
AM19	439	311	0.35	−29.05	−0.35	−4.11	−0.89	−4.95
AM20	435	205	0.2	−28.55	−0.31	−4.01	−0.44	−4.52
AM21			0.03		−0.12	−3.63	−0.68	−4.34
AM22			0.03		0.25	−3.81	0.07	−3.86
AM23			0.03		1.23	−2.73	0.47	−3.2
AM24			0.04		0.05	−3.7		
AM25					0.88	−2.99		
AM26			0.04		1.32	−2.69		
AM27					1.26	−2.62		
AM28			0.03		1.22	−2.77		
AM29					1.48	−2.81		
AM30			0.02		1.7	−2.28		

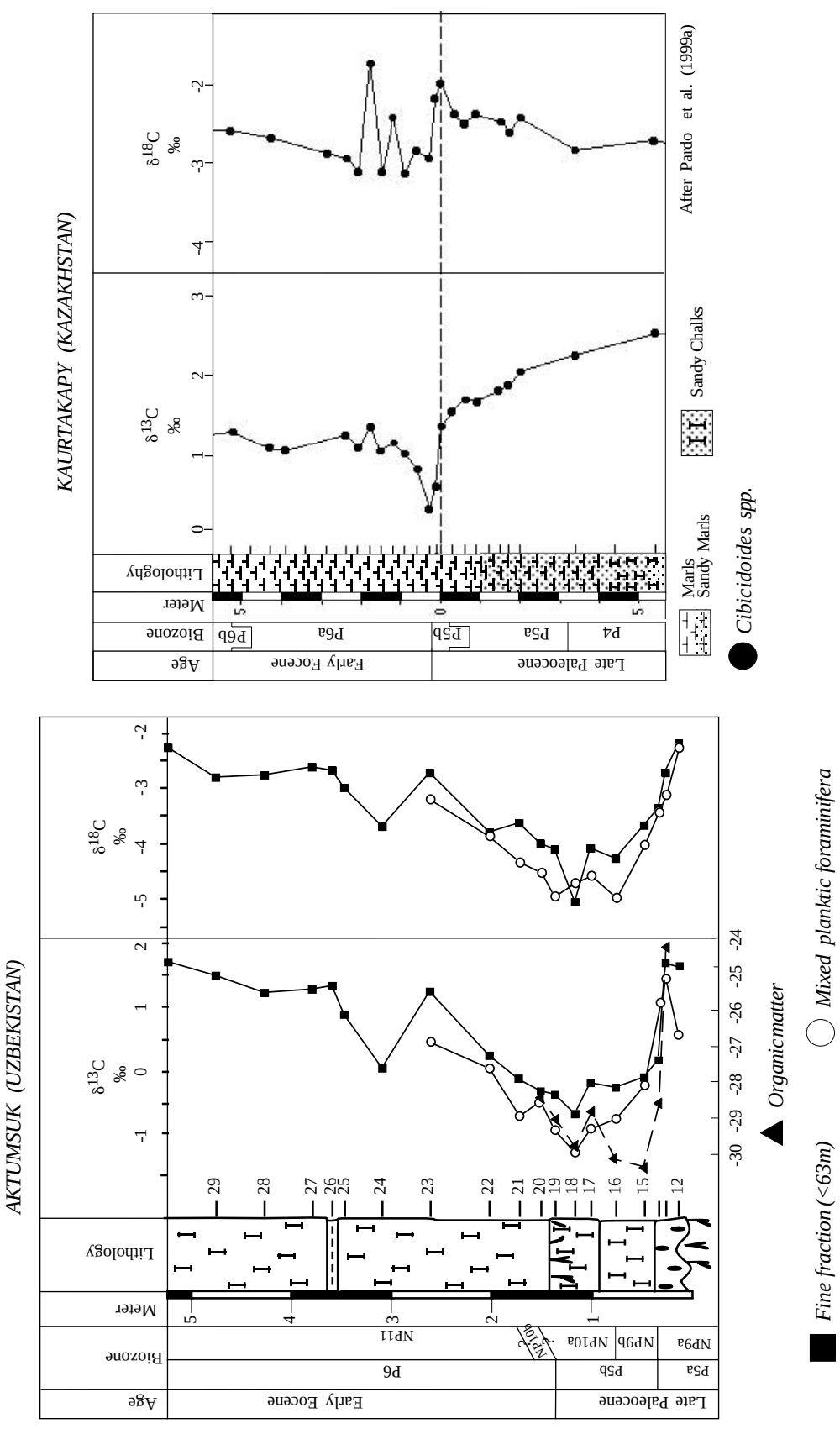

Fig. 12 Carbon and oxygen isotope records across the Paleocene–Eocene transition at Aktumsuk (Uzbekistan) and Kaurtakapy (Kazakhstan). At Aktumsuk, stable isotopes analyses were conducted on the fine fraction (< 63 μm), on mixed planktic foraminiferal assemblage and on organic matter content (see Table 1 for $\delta^{13}C$ and $\delta^{18}O$ values). At Kaurtakapy analyses were conducted by Pardo et al. (1999a, 1999b) on benthic foraminifer *Cibicidoides* spp. See Fig. 5 for symbol explanation at Aktumsuk. The lithologic log of Kaurtakapy is from Pardo et al. (1999a)

At Kaurtakapy the $\delta^{18}O$ record is highly variable. In the upper Paleocene (Zones P4b and P5a) $\delta^{18}O$ values average −2.6‰ but increased to −2.2‰ in Subzone P5b. Coincident with the $\delta^{13}C$ shift and the rapid increase in warm-water species (Pardo et al. 1999a), $\delta^{18}O$ values decrease by 1‰. In P6a, $\delta^{18}O$ values average −2.8 to −3‰, except for two peaks which reach −2.4 and −1.7‰, respectively (Fig. 12).

Organic geochemistry

Organic matter abundance and origin

Kaurtakapy sediments are poor in organic matter (<0.17 %) except for the brown clay layer (sample 162) which reaches 0.4 % (Fig. 9): Values <0.2 % are considered background amounts, consisting of highly refractory organic carbon. In contrast, at Aktumsuk, sediments from the P5b interval have a very high organic content, reaching a maximum of 8.44 % (Fig. 9; Table 1) that coincides with the onset of the carbon isotopic excursion in carbonates and planktic foraminifera (Fig. 12). Detailed molecular organic geochemical studies of the lipid fraction within this black shale unit (samples AM14 to AM18) revealed that the organic matter originated mainly from planktonic and bacterial sources with a strong overprint of bacterial recycling (data not shown). This assumption is supported by relatively high hydrogen index values that typically range from 300 to 400 mg HC/g TOC in the organic-rich layer (AM 13 to AM 19; Table 1). Values in this range characterize a type-II kerogen of predominantly marine origin (Tissot and Welte 1984). Among the observed lipids from marine primary producers we found loliolide, a compound that was previously observed in sediments underlying high productivity areas (Hinrichs et al. 1999b), dinosterol derived from dinoflagellates (Boon et al. 1979), 4,24-dimethylcholestan-3-one (Gagosian and Smith 1979), and 6,10,14-trimethylpentadecan-2-one, a product in the early diagenetic alteration pathway of phytol. Strong bacterial contributions to sedimentary organic matter are evident from abundant series of hopanoids (alcohols, carboxylic acids, ketones, and hydrocarbons) and archaeol, with the hopanoids being the most abundant compound class in the lipid fraction. Contributions of terrestrial organic matter are indicated by biomarkers that are diagnostic for terrestrial higher plants, namely friedelanone and a series of long chain fatty acids (C_{22}–C_{30}) with an even-over-odd carbon number preference. The occurrence of these biomarkers is consistent with the macroscopic observation that land plants remain within the organic-rich layer. Ultimately, the presence of lycopane is indicative of anoxic to suboxic water column conditions, as prevailing in the Cariaco Trench, where this compound is particularly abundant in waters below the oxic-anoxic interface (Wakeham 1990).

The absence of thermal alterations that might have significantly altered the isotopic composition of the organic matter is indicated by the predominance of chemically functionalized compounds in the lipid fraction. For example, sterenes and hopenes, compounds generated during early diagenesis from their oxygenated precursors, are only minor constituents in the lipid fraction. This interpretation is consistent with Rock Eval T_{max} values between 376 and 439 °C indicative of immature organic material (Table 1).

Organic records at the LPTM

$\delta^{13}C$ TOC declines drastically at the base of the organic carbon-rich black shale by more than 5‰ from −24.30‰ in sample AM 13 to a minimum of −30.35‰ in sample AM 15 (Fig. 13; Table 1). With the exception of sample AM 17, $\delta^{13}C$ values remain low up to sample AM 19 and increase to −28.55‰ in sample AM 20. This decline is interpreted to reflect both, the drastically changed conditions for organic matter preservation, leading to the burial of more labile organic matter that was isotopically depleted, and an increasing depletion in ^{13}C in the inorganic carbon pool in surface waters overlying the site during time of burial. Secondary isotopic fractionations during diagenesis can account for up to 3‰ alteration of the original signal (Hayes et al. 1989). Carbon isotopic ratios of individual compounds of primary production are thought to be less influenced by diagenetic alteration and therefore can be used to assess the carbon isotopic composition of the organic matter derived from photosynthetic processes (Hayes 1993). Effects of diagenesis on the isotopic compositions of individual biomarkers can be neglected, even when the functionality of these compounds is modified by chemical or microbial transformations under conservation of the original carbon skeleton (Hayes et al. 1989). The study of carbon isotopic compositions of individual biomarkers can thus be applied to reconstruct biogeochemical processes in ancient environments.

A depletion of ^{13}C in the oceanic and atmospheric carbon dioxide pools is indicated by minimum $\delta^{13}C$ of 4,24-dimethylcholestan-3-one and friedelanone in sample AM 16. 4,24-Dimethylcholestan-3-one and friedelanone as two source-specific markers were selected for analytical reasons, since they met the resolution requirements for compound-specific isotopic analysis. 4,24-Dimethylcholestan-3-one could be derived from a 4,24-dimethylsterol by an early diagenetic transformation (Gagosian and Smith 1979). 4-methylsteroids are commonly interpreted as markers for dinoflagellates (e.g., Robinson et al. 1984). More recent studies have extended the range of possible producers to prymnesiophytes (Volkman et al. 1990) and diatoms (Volkman et al. 1993).

The record of 4,24-dimethylcholestan-3-one suggests that the isotopic excursion observed in carbona-

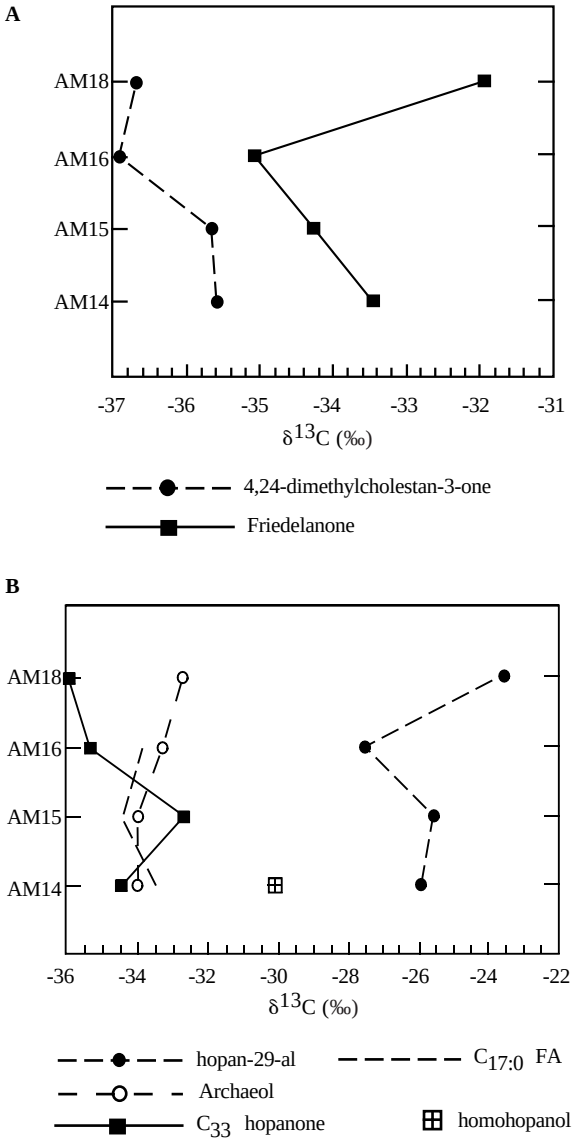

Fig. 13 **A** Organic carbon isotope records of biomarkers from higher land plants and marine algae in the Subzone P5b interval at Aktumsuk, Uzbekistan. **B** Organic carbon isotope records of bacterial biomarkers from Subzone P5b at Aktumsuk

ceous components and organic carbon (Table 1) is indeed consistent with a depletion of ^{13}C in dissolved CO_2 in surface waters. At the same time, the decrease in the higher land plant marker reflects ^{13}C depletion in atmospheric CO_2. $\delta^{13}C$ decreases by approximately 2‰ from sample AM 14 to AM 16. A similar observation was made by Kaiho et al. (1996) in the Taiwanui P–E section. These authors report a 2.8‰ excursion of the higher land plant wax component n-$C_{29}H_{60}$.

To a certain degree, other studied biomarkers appear to record the negative excursion of isotopes, particular bacterially derived hopanoids, 17β (H)-*trihomo*-hopanone, and a tentatively identified hopan-29-al (Fig. 13 B). Relatively heavy values of the latter compound suggest its derivation from autotrophic organisms, e.g., cyanobacteria.

Discussion

Primary original signal vs secondary diagenetic signal in the isotopic record

The co-variance of carbon and oxygen isotopes may be linked through paleoceanographic cause-and-effect. However, stratigraphic sample-by-sample covariance of $\delta^{18}O$ and $\delta^{13}C$ can often indicate the presence of diagenetic alteration due to recrystallization of carbonate in the presence of meteoric water (which is depleted in ^{18}O) and which is carrying ^{12}C derived from organic matter (Corfield et al. 1991). Moreover, Oberhänsli et al.(1998) have shown that in Kazakhstan the Cretaceous–Paleogene transition sediments, particularly chalks which were deposited in shallow environments, undergo more drastic diagenetic alteration than deep-water carbonates. Carbonate sediments in a shallow-water epicontinental sea are particularly vulnerable to postdepositional alteration processes. Both dissolution and recrystallization are processes which may have altered the primary stable isotopic composition.

At Aktumsuk the relatively shallow depositional environment in combination with the excellent correlation between $\delta^{18}O$ and $\delta^{13}C$ for isotope data (r=0.94; Fig. 14) suggests that the primary isotope signal measured on the fine fraction could be partly altered during early diagenesis.

Scanning electron microscopic observations on manually fractured tests of planktic foraminifera reveal that the interior chambers and the small pores of the test walls are generally free of secondary calcite (Fig. 7); however, some calcite tests, particularly in the P5b interval, are affected by dissolution–recrystallization processes and by secondary calcite overgrowth (Fig. 8) which may account for the light planktic foraminiferal $\delta^{18}O$ values (−2.28 to −4.95‰; Fig. 12). Pardo et al. (1999a) explained the relatively low $\delta^{18}O$ values (−3 to −1.7‰) at Kaurtakapy as the result of

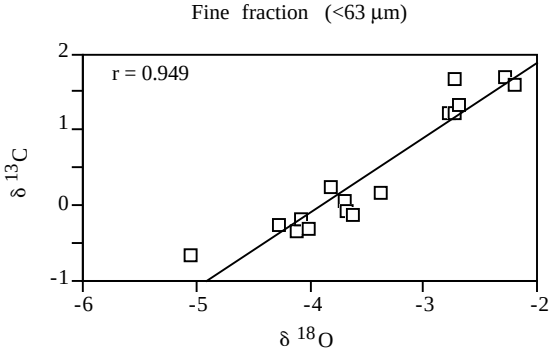

Fig. 14 Correlation of $\delta^{18}O$ and $\delta^{13}C$ values from the fine fraction (< 63 μm) in the Aktumsuk section, Uzbekistan

diagenetic alteration without, however, excluding possible salinity effects which may have affected the $\delta^{18}O$ signal.

Thus, no reliable paleotemperature interpretations based on oxygen isotope ratios can be used in either the Aktumsuk or Kaurtakapy sections. However, similar to Kaurtakapy (Pardo et al. 1999a), minimum $\delta^{18}O$ values which indicate warming coincide with the P5b interval (Fig. 12) and the incursion of a warm planktic foraminiferal species (i.e., acarininids, igorinids, and morozovellids). These two concomitant events suggest that although the oxygen isotopic record is partly altered, the general trend of the signal is preserved. The negative $\delta^{18}O$ shift observed in Subzone P5b (Fig. 12) may be related to the prominent warming that affected deep and high-latitude surface waters at the end of the Paleocene.

At Aktumsuk high organic matter content coincides with minimum $\delta^{13}C$ values in Subzone P5b (Figs. 9, 12). Diagenesis of organic material, strongly depleted in ^{13}C, could have partly induced the negative $\delta^{13}C$ excursion observed in the fine fraction at the end of the Paleocene. Moreover, the significance of the negative $\delta^{13}C$ shift observed in the planktic foraminifera (Fig. 12) must also be considered carefully. Actually minimum $\delta^{13}C$ values recorded in Subzone P5b coincide with a degradation of planktic foraminiferal preservation. In this interval calcite tests are commonly recrystallized with diagenetic calcite of questionable origin; foraminiferal $\delta^{13}C$ values are probably partly related to the diagenetic calcite phases. Nevertheless, similar carbon isotopic trends in the fine fraction, in the planktic foraminifera, and in organic carbon components (Figs. 12, 13) suggest that at least part of the $\delta^{13}C$ shift observed is related to the LPTM. However, as most of geological sections from widespread location show the same pattern of isotopic change during the LPTM (see Introduction), it is difficult to concede that the general trend of the signal observed at Aktumsuk is only caused by local diagenetic alteration.

Late Paleocene Thermal Maximum

During the Late Paleocene, the marginal northeastern Tethys is marked by coincident negative $\delta^{13}C$ shifts recorded in calcite of benthic foraminifera (*Cibicidoides* spp.) at Kaurtakapy and mixed planktic foraminifera at Aktumsuk (Fig. 12). These two negative shifts suggest that a major change of $\delta^{13}C$ affected the water column in the marginal epicontinental sea. The rapid $\delta^{13}C$ excursion affected not only the oceanic but also the atmospheric pool, as indicated by the ^{13}C-depletion observed in friedelanone, a useful tracer for terrestrial vascular plants (Figs. 13A, 15). At Kaurtakapy the rapid $\delta^{13}C$ shift is preceded by a gradual decrease in $\delta^{13}C$ values which has not been observed at Aktumsuk because of the presence of a major hiatus that encompasses the Maastrichtian and most of the Paleocene (Fig. 12). At Aktumsuk the $\delta^{13}C$ excursion has an amplitude of approximately 2.5‰, whereas at Kaurtakapy, the relatively smaller $\delta^{13}C$ shift (1.1‰) may be due to a hiatus at the sharp lithological contact between the clay layer and the overlaying marls that removed the lower part of the $\delta^{13}C$ excursion.

In both sections the $\delta^{13}C$ shift coincides with minimum $\delta^{18}O$ values and a rapid diversification of warm-water planktic foraminifera. At Aktumsuk this subtropical incursion is characterized by maximum igorinid abundance (Pardo et al. 1999b) in contrast with the acarininid and morozovellid peaks that generally occur in low latitude, at Kaurtakapy (Pardo et al. 1999a), in other Tethys sections (Lu et al. 1995, 1996, 1998a; Arenillas and Molina 1996) and in the Pacific Ocean (Kelly et al. 1996; Bralower et al. 1995).

Methane-blast hypothesis

A seriously considered mechanism for the negative carbon isotopic excursion during the LPTM was the release of ^{13}C depleted methane from oceanic methane clathrates as a consequence of oceanic deep-water warming, which possibly led to destabilization of clathrates in sediments in a water depth range of 900–1400 m (Dickens et al. 1995, 1997). Modern analogs of decomposing hydrates have been shown to contain biomarkers that are diagnostic for the process of anaerobic methane oxidation (Hinrichs et al. 1999a), an important biogeochemical process in marine anoxic sediments and anoxic water columns (e.g. Reeburgh 1976). In contrast, under oxic conditions, methane is oxidized by methanotrophic bacteria, a group of microorganisms which also can be recognized by specific biomarkers (Summons et al. 1994). The shallow paleowater depth at the Aktumsuk site excludes an in situ release of methane from clathrates. However, methane released in deeper waters along the Uzbekistan continental margin could have reached the site of investigation, where methanotrophic processes might have occurred. In such a case the anoxic water column would have favored the preservation of biomass formed by these methanotrophic processes.

In organic-rich samples from the Aktumsuk section, several compounds were identified that potentially originated from methanotrophic organisms. These compounds include archaeol, an archaea-specific biomarker that was previously found in several modern gas seep environments (Hinrichs et al. 1999a; Hinrichs et al. 1999). In these studies a strong depletion in ^{13}C ($\delta^{13}C \leq -100‰$) revealed that it was produced anaerobically by archaea that were utilizing methane as their carbon source. Similarly, ^{13}C-depleted hopanoid compounds ($\delta^{13}C \sim -80‰$) would be indicative of aerobic methanotrophy (e.g., Freeman et al. 1990). However, relatively heavy carbon isotopic compositions of above mentioned compounds (Fig. 13B) indi-

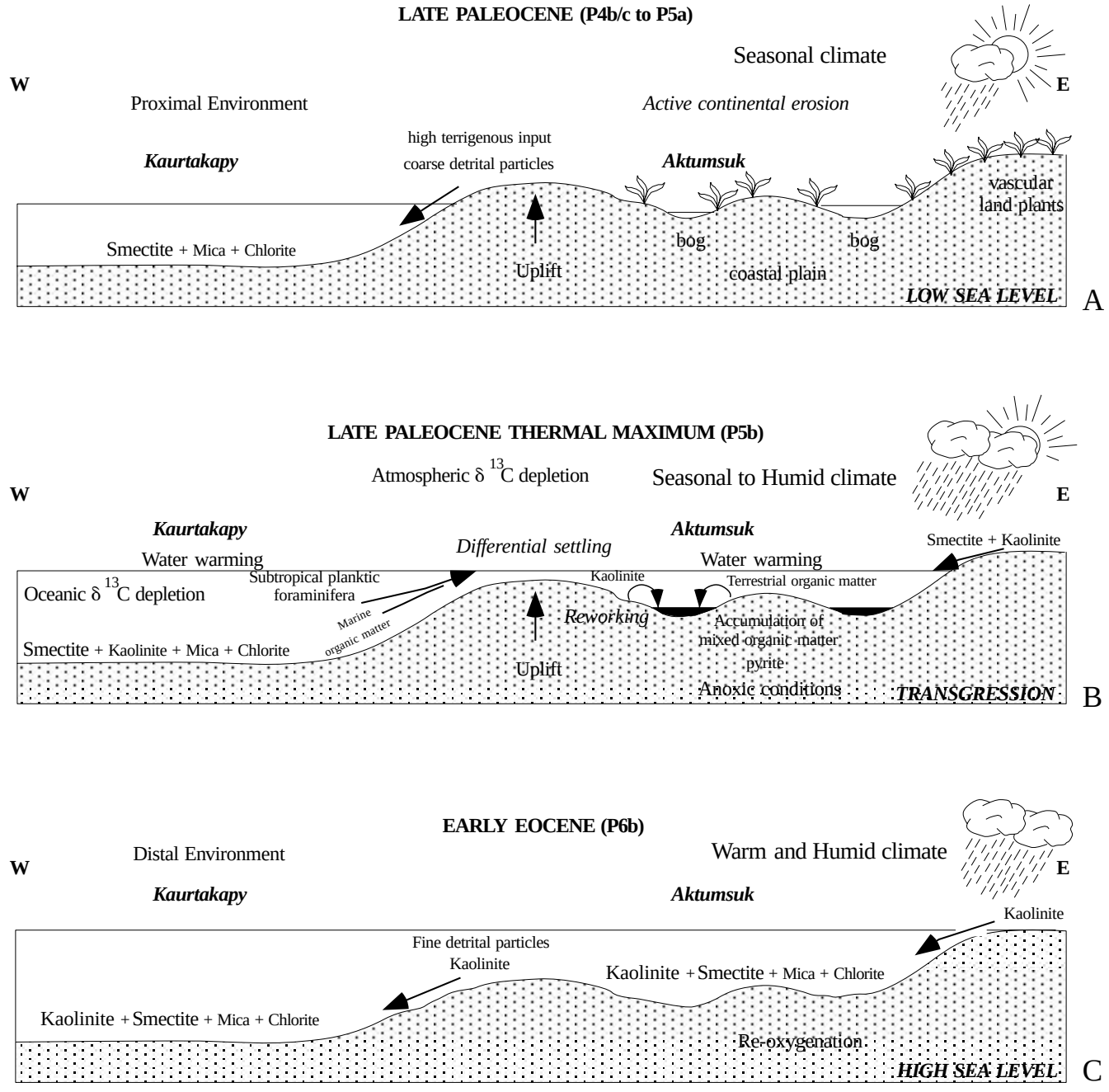

Fig. 15A–C Conceptual model of the possible climatic and environmental events. **A** During the Late Paleocene (Subzones P4c and P5a); **B** during the Late Paleocene Thermal Maximum (Subzone P5b); **C** during the Early Eocene (Zone P6) in the marginal northeastern Tethys

cate that their biological producers utilized carbon sources other than methane. $\delta^{13}C$ values of archaeol indicate its derivation from methanogenic bacteria, whereas the scatter of ^{13}C values of hopanoids indicates at least a mixture of two different non-methanotrophic microbial sources (Fig. 13B). Notably, homohopanol derived from chemical cleavage of bacteriohopanepolyol, which is potentially derived from methanotrophic bacteria (Summons et al. 1994), has a $\delta^{13}C$ composition of $\sim -30‰$. This relatively heavy isotopic signal indicates that a contribution of methanotrophic bacteria does not exist or can be neglected.

Low calcite content

Various processes can result in low calcite content, including decreased productivity of calcareous microplankton, high detritus, and/or phyllosilicate input during sea level fluctuations, dilution, and carbonate dissolution.

At Kaurtakapy the low sea levels corresponding to the upper part of Zone P4c and Zone P5a (Haq et al. 1988) may account for the observed low carbonate sedimentation as a result of increased terrigenous input associated with increased continental erosion and hence dilution of carbonates in this basin (Fig. 4). In this section the P–E event is marked by a concomitant decrease in calcite from 60 to 30 % and in $\delta^{13}C$ values (Figs. 4, 12). Contrary to the rapid post-$\delta^{13}C$ shift recovery, calcite content remains low through the P6a interval starting to increase only in the P6b interval (Figs. 4, 12). These observations suggest that two distinct events are responsible of the low calcite content. The simultaneous decrease in calcite and $\delta^{13}C$ values could be related to the global changes that characterized the LPTM. In nearly all published P–E records the negative $\delta^{13}C$ excursion coincides with an apparent global reduction in carbonate accumulation as evidenced by carbonate dissolution and/or hiatuses, over a wide depth range from continental margins to abyssal basins (e.g., Kennett and Stott 1990; O'Connell 1990; Lu and Keller 1993, 1995; Lu et al. 1996, 1998a, 1998b; Thomas and Shackleton 1996; Bolle et al. 1998). Addition of massive amounts of carbon from oxidized methane hydrate (Dickens et al. 1995) has been invoked to explain this carbonate reduction; however, cause(s) and mechanism(s) of this reduction are not yet well understood. The reduced carbonate accumulation persisting above the P–E event coincides with a high content of phyllosilicates suggesting increased input of fine detrital particles into the Kaurtakapy basin during the high sea level period, following the sea level rise which marked the end of the Paleocene (Haq et al. 1988).

During the low sea level periods corresponding to the upper part of P4c and P5a (Haq et al. 1988), Kaurtakapy was located relatively close to the source of the terrigenous material as indicated by an increase in coarser particles of quartz, plagioclase, and potassic feldspar (>16 μm; Figs. 4, 15). During the high sea level period that characterized the base of the Ypresian, the Kaurtakapy section was located in a more distal environment, sufficiently distant from the continental source to deposit mainly finer detrital particles (phyllosilicates; <2 μm; Figs. 4, 15).

At Aktumsuk, the Late Paleocene is marked by a slight decrease in calcite with a minimum in calcite values (42 %; sample 15) preceding the maximum of the negative $\delta^{13}C$ excursion (Figs. 5, 12). Traces of dissolution affecting foraminiferal tests have only been observed in Subzone P5b, suggesting that carbonate dissolution is responsible mainly for the relatively low calcite content during the LPTM.

Anoxic event during the LPTM

The Upper Paleocene organic-rich layer has been described in Central and South Asia, Caspian region, and the Caucasus (Gavrilov and Muzylev 1991; Gavrilov et al. 1997). This horizon enriched in organic matter can be attributed to a single narrow stratigraphic interval correlatable over vast areas, in southern Turkmenia, in the Precaspian, and in the Tadzhik Depression (Gavrilov and Muzylev 1991; Muzylev et al. 1994). This sapropelite event corresponds to the organic-rich interval observed in Subzone P5b at Aktumsuk (Fig. 12). According to these authors, the accumulation of the isochronous organic-rich sediments took place near the base of a short-lived and quite rapid eustatic transgression during the Late Thanetian time.

At the end of the Paleocene, the western part of Uzbekistan was affected by a widespread transgression, recognized on a global scale (Haq et al. 1988). This transgressive event marked the first invasion of marine waters rich in nutrients onto a continental area (Fig. 15B). Field observations have shown that on a short distance (~ 50 km) in the cliffs along the Aral Sea coast, the erosive surface is at different depths below this sapropelite unit suggesting an irregular local topographic configuration. At Aktumsuk, the erosion of the sediments (e.g., major hiatus) modeled a paleo-relief with depressions, which may have favored the preservation of organic matter. The topographic lows may have locally inhibited bottom-water circulation and allowed isolated pockets of stagnant water to maintain anaerobic conditions (Hallam and Bradshaw 1979). Slow circulation intensity (Wetzel 1991) and high organic material input (Calvert 1987) controlled the oxygenation at the sea floor leading to the formation of an oxygen-depleted environment. This environment favored the formation of reduced minerals such as pyrite. At Aktumsuk, the co-existence of pyrite and an organic-rich layer indicates that low oxygen conditions prevailed during Subzone P5b. The presence of lycopane suggests that during the deposition of organic-rich layer significant parts of the water column were suboxic to anoxic. The redox conditions in the water column facilitated preservation of organic matter. Part of the organic-rich layer is characterized by low-angle cross bedding (Fig. 12). Gavrilov et al. (1997) suggest that this particular feature could have been induced by the accumulation of sediments in the proximal zone of uplift under a relatively active hydrodynamic regime; however, this interpretation seems inconsistent with the suboxic to anoxic conditions which prevailed in the water column at this time. Another hypothesis would be that the organic material has been slightly transported by lateral currents and reworked from a topographic low into another one; however, this interpretation remains speculative.

The sea level fluctuations over the marginal northern part of the Tethys created favorable sites for the accumulation and preservation of organic-rich sediments; however, this depends mainly on local topographic configuration. At Kaurtakapy the absence of

major erosion of the sediments (no major hiatus) suggests a large basin floor, but without steep relief, which may have limited the accumulation and preservation of organic matter. However, in this section the higher organic matter (0.4 %) content was measured in Subzone P5b in the 10 cm thick brown clays which contains fish debris and pyrite nodules, suggesting that low oxygen conditions (i.e., hypoxia) prevailed also during the Late Paleocene at Kaurtakapy.

During the Early Eocene (Subzone P6a), anoxic conditions were probably terminated by increasing water circulation. This may be due to tectonic movements that changed the configuration of the basin, relative eustatic fluctuations, climatic changes, and/or opening seaways (Wetzel 1991). The opening of an important oceanic channel to the north with the Arctic Ocean and the reduction of emerged lands to the southeast (Fig. 3) could have been the main mechanism of the re-oxygenation of the Aktumsuk basin during the Early Eocene (Fig. 15). The return to more oxic conditions is indicated by the absence of organic matter and pyrite in the early Eocene sediments of Aktumsuk (Fig. 12; Table 1).

Significance of clay minerals

Detrital input is the dominant factor responsible for clay mineral distribution in marine sediments. Mica, chlorite, associated quartz, and feldspars typically constitute terrigenous species (Chamley 1998). These clay minerals develop generally in areas of steep relief where active mechanical erosion limits soils formation, particularly during periods of high tectonic activity. They can also form in cold and/or desert regions where low temperatures and/or low rainfall reduce the chemical weathering (Millot ; Chamley 1998).

During the Early Eocene and at times in the Paleocene, peaks of volcanic activity have been recorded on the active margin of Eurasia. For the first time in Cenozoic history, volcanic belts can be traced continuously from the Rhodope massif to Afghanistan, via the southern Caspian Sea coast (Kazmin et al. 1986). Despite this intensive calc-alkaline volcanism to the south of the studied area, no volcanoclastic components were observed throughout the sedimentary column at Aktumsuk and Kaurtakapy. This observation suggests that smectite is not derived from the weathering of volcanic materials (Chamley 1998). In the studied area this clay mineral appears to be mostly of detrital origin and can issue from soils developed under a warm to temperate climate characterized by alternating humid and arid seasons (Chamley 1998).

In Antarctica, the South and North Atlantic (Robert and Chamley 1991; Robert and Kennett 1992, 1994; Gibson et al. 1993; Knox 1996; Gawenda et al. 1999), and in several Tethyan sections (Lu et al. 1998a; Bolle et al. 1999), the LPTM is marked by the appearance, or a strong increase, in kaolinite. The high kaolinite content has been interpreted as marker of humidity. This clay mineral develops typically in tropical soils which are characterized by warm, humid climates, well-drained areas with high precipitation, and accelerated leaching of parent rocks (Robert and Chamley 1991).

At Aktumsuk the P5b interval is marked by increased kaolinite (Figs. 11, 16) which could be related to the humid episode that affected mainly high-latitude areas and the North Atlantic during the latest Paleocene. However, the climatic significance of kaolinite must be considered carefully in this section. Clay mineral assemblages (smectite, mica, chlorite, kaolinite, and IS) are similar in the Late Paleocene sediment (P5a/b) and in the underlying Campanian chalks (Fig. 16). The main difference is the kaolinite and smectite contents, which are higher in the P5b interval (12 and 10 %) than in the Campanian (7 and 2 %). Thus, part of the clay minerals observed in the P5b interval could have been introduced into marine sediments through erosion of both older sediments and soils during the sea level transgression that took place at the end of the Paleocene in this region (Gavrilov et al. 1997); hence, both kaolinite and smectite could be reworked from Late Cretaceous sediments.

However, kaolinite and smectite observed in the P5b interval are not only reworked from older soils and sediments. All Late Paleocene samples contain rare reworked Campanian nannofossils suggesting minor reworking at this time. Moreover, the P5b interval is marked by decreased grain size as suggested by a high quartz (<2-μm size fraction) / quartz (2- to 16-μm size fraction) ratio, and the relatively low plagioclase and potassic feldspar contents of the 2- to 16-μm size fraction (Fig. 16). This major sedimentological change implies different terrigenous sources during the Late Paleocene transgression and the Campanian (Fig. 16). These observations could indicate that part of the kaolinite comes from contemporaneous paleosoils and could suggest humidity on the adjacent land areas during the Late Paleocene. At Kaurtakapy the P6b interval is marked by a relatively strong increase in kaolinite and high kaolinite/smectite ratio (Fig. 10). The sporadic presence of kaolinite from the underlying layers and the low kaolinite content during the Late Paleocene transgressive event, where a maximum of reworking could be expected, suggest that this mineral may be used in this case as a climatic factor.

Paleolandscape and climate

The sea level rise affecting the marginal northeastern Tethys at the end of the Paleocene was preceded by a regressive period which is indicated at Aktumsuk by the presence of an important hiatus and erosive overlapping of older sediments (Campanian) by the Late Thanetian sediments. As a result of the regression,

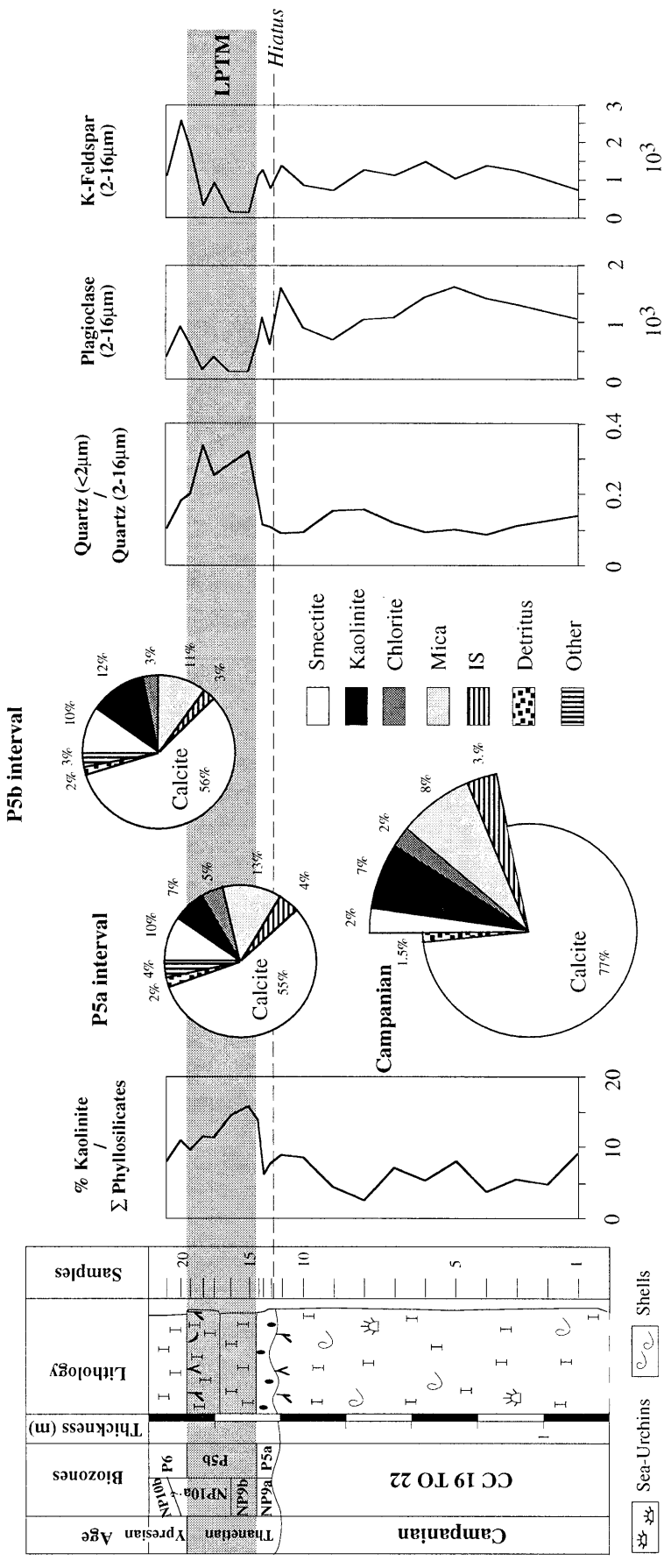

Fig. 16 Mineralogical composition of Campanian chalks and the Thanetian sediments, plagioclase and potassic feldspar variations of the 2- to 16-µm size fraction and quartz (<2-µm size fraction)/quartz (2- to 16-µm size fraction), and kaolinite/Σ phyllosilicates ratios at Aktumsuk (Uzbekistan). Except plagioclase and K-Feldspars, which are given in counts per minute, other minerals are given in relative percent abundance. The ratios are calculated from XRD mineral peak data in counts per minute. See Fig. 5 for symbol explanation

large coastal lowlands developed along the periphery of a relatively shallow, epicontinental sea and around archipelagos (Gavrilov et al. 1997). The emergent areas were characterized by formation of lakes and waterlogged sectors (lacustrine bog landscape) on newly developed coastal plains (Fig. 15A; Gavrilov et al. 1997).

The abundance of smectite in the marine sediments of Kaurtakapy in Zone P4 and Subzone P5a (Fig. 10) suggests the dominance of a temperate to warm climate with humid and arid seasons in the source areas (Fig. 15A). This seasonal climate is consistent with the formation of bogs on the coastal plains. Most of the modern well-developed bogs are found in the temperate regions of North Europe, West Siberia, and North America (Schneider and Schneider 1974). Judging from the present-day analogs, the formation of peat bogs during the period of low sea levels preceding the Late Paleocene transgressive event required a temperate climate with alternating humid seasons. At Kaurtakapy smectite is associated mainly with relatively high mica and chlorite contents (Fig. 10). Such a clay detrital assemblage could reflect the combined influences of land petrography and continental climate. In temperate regions the petrographic influence of rocky substrates is often reflected by the so-called primary minerals such as mica and chlorite, whereas the petrographic input from pedogenic blankets is marked mostly by irregular mixed-layers, kaolinite, and smectite (Chamley 1989).

The end of the Paleocene is characterized by a general transgression with a sea level rise of several dozens of meters (Gavrilov et al. 1997). At Aktumsuk the transgression was rapid and predated slightly the accumulation of the organic-rich layer. The first deposits related to the transgressive phase are poor in organic matter ($< 0.4\,\%$) and correspond to Subzone P5a interval (Fig. 9). However, the occupation by sea was not synchronous everywhere. For instance, the transgression affected the Northern Caucasus only at the end of Zone P5b; consequently the base of the sapropelite unit is missing (Muzylev et al. 1996).

At Aktumsuk the sea level rise is marked by an incursion of marine waters onto a continental area (Fig. 15B). These waters were enriched in nutrients, detrital clay minerals, and Campanian nannofossils stemming from the erosion of older sediments and soils. The irregular topography developed by the erosion created favorable sites to trap organic matter and clay minerals. The marine material is mixed in the deposits with the terrestrial organic matter, which was concentrated in soils and in peat bogs. At Kaurtakapy the sea level rise is marked by a lithological change from marls to clays (Fig. 4). The sharp contact observed between the two lithologies suggests a break in sedimentation and/or condensation which corresponds probably to the maximum transgression.

Inferred from minimum $\delta^{18}O$ values (Fig. 12), seawaters of the marginal northeastern Tethys warmed up at the end of the Paleocene. This seawater warming, characteristic of the LPTM, was associated with the rapid sea level rise and favored the incursion of transient subtropical planktic foraminiferal fauna in the epicontinental northeastern basin (Fig. 15B). The subtropical incursion is characterized by maximum igorinid abundance at Aktumsuk (Pardo et al. 1999b) and by the dominance of acarininids and morozovellids at Kaurtakapy (Pardo et al. 1999a).

Compared with lower-latitude Tethys sections (southern Spain and northern Tunisia; Lu et al. 1998a; Bolle et al. 1999) and North Atlantic sections (Gibson et al. 1993; Knox 1996; Gawenda et al. 1999), the marginal northeastern Tethys does not appear to be affected during the LPTM by a major humid episode marked by strong kaolinite influx. At Aktumsuk part of the relatively high kaolinite content in Subzone P5b (Figs. 11, 16) may be the result of erosion from older sediments as well as from reworking during the sea level transgression and accumulation in favorable sites. During this period the abundance of smectite and the very low kaolinite content observed at Kaurtakapy suggest the dominance of a seasonal climate on the adjacent land areas (Fig. 10). However, we cannot exclude that the warm and humid climatic conditions were already initiated on the adjacent land areas at the end of Paleocene. At Aktumsuk it has been shown that part of the kaolinite could come from coeval paleosoils, whereas at Kaurtakapy the low kaolinite and the high smectite contents could result by enrichment trough differential settling. In periods of sea level rise, kaolinite, chlorite, and mica are deposited close to shorelines, whereas smectites are transported away from shores (Gibbs 1977; Adatte and Rumley 1989).

During the Early Eocene (Zone P6), the marginal northeastern Tethys is marked by a period of high sea level (Haq et al. 1988), increasing water circulation leading to the re-oxygenation of the basin and a climatic change (Fig. 15C). During this sea level highstand, sedimentation is dominated mainly by fine detrital particles (phyllosilicates) in the Kaurtakapy and Aktumsuk sections (Figs. 4, 5), indicating deposition in a distal environment, relatively far from the continental source. At Aktumsuk the relatively high kaolinite content in Zone P6, and at Kaurtakapy the high kaolinite/smectite ratio observed in Subzone P6b, suggest increased humidity in the source areas of the marginal northeastern basin (Figs. 10, 11). Most likely, warm and humid climate initiated during the Late Paleocene extended during the Eocene onto adjacent land areas of the basin (Fig. 15C).

Conclusion

Based on sedimentological, faunal, mineralogical, and geochemical criteria, the following conclusions are drawn:

1. During the LPTM, the marginal northeastern Tethys is marked by a negative $\delta^{13}C$ excursion, minimum $\delta^{18}O$ values, and a rapid diversification of warm-water planktic foraminifera.
2. TOC and biomarker isotopic data are consistent with a 2–3‰ depletion of oceanic and atmospheric CO_2 pools.
3. No biomarker products of methanotrophic organisms that were related to a potential methane release were observed at the Uzbekistan continental margin. This observation does not exclude the possibility of a methane release at a remote location.
4. At the end of the Paleocene, the marginal northeastern Tethys is affected by a widespread transgression. At Aktumsuk this transgressive episode is marked by the incursion onto a continental area of high productivity marine waters.
5. The irregular topographic configuration of the Aktumsuk site favored the accumulation of organic matter. Biomarker distributions and hydrogen indices indicate an organic matter composition predominantly of marine algae and bacteria with admixtures of terrestrial carbon.
6. The presence of lycopane indicates that significant parts of the water column were suboxic to anoxic during the deposition of the organic-rich layer.
7. Clay mineral distribution indicates the dominance of a temperate to warm climate with wet and arid seasons during the Late Paleocene (Subzones P4 and P5a). Warm and humid climate initiated during the LPTM (Subzone P5b), extended during the Eocene (Zone P6).

Acknowledgements We thank H. Oberhänsli (Alfred Wegener Institute, Potsdam, Germany) for the sampling of the Kaurtakapy section, Kazakstan, and for coming with us in the field in Uzbekistan (INTAS project with T. Adatte). We also thank J. Zachos (Santa Cruz University, California), J.M. Hayes (WHOI), and R. Summons (AGSO) for discussions. We thank J. Richard for conducting X-ray preparations at the laboratory of mineralogy and petrology, and P. Steinmann and S. Ryser for conducting Rock Eval analyses at the GEA laboratory, University of Neuchâtel, Switzerland. This study was supported by the Swiss National Foundation, grant no. 2100-043450.95/1 (to M.-P. Bolle), and DGES grant no. Pb 97-1016 (to A. Pardo). K.-U. Hinrichs was supported by a research fellowship from the "Deutsche Forschungsgemeinschaft." Laboratory expenses for organic geochemical analyses were supported by NASA.

References

Adatte T, Rumley G (1989) Sedimentology and mineralogy of Valanginian and Hauterivian in the stratotypic region (Jura mountains, Switzerland). In: Wiedmann J (ed) Cretaceous of the Western Tethys. Proc 3rd Int Cretaceous Symp, Tübingen, Germany, 1987, pp 329–351

Arenillas I, Molina E (1996) Bioestratigrafia y evolucion de las asociaciones de foraminiferos planctonicos del transito Paleoceno-Eoceno en Alamedilla (Cordilleras Béticas). Rev Esp Micropal 18:75–96

Aubry MP (1996) Towards an Upper Paleocene–Lower Eocene high resolution stratigraphy based on calcareous nannofossil stratigraphy. Israel J Earth Sci 44:239–253

Axelrod DI (1984) An interpretation of Cretaceous and Tertiary biota in polar regions. Palaeogeogr Palaeoclimatol Palaeoecol 45:105–147

Berggren WA (1969) Cenozoic chronostratigraphy, planktonic foraminiferal zonation and the radiometric time scale. Nature 224:1072–1075

Berggren WA, Miller KG (1988) Paleogene tropical planktic foraminiferal biostratigraphy and magnetobiochronology. Micropaleontology 34:362–380

Berggren WA, Kent DV, Swisher CC III, Aubry MP (1995) A revised Cenozoic geochronology and chronostratigraphy. SEPM Spec Publ 54:129–213

Blow WH (1979) The Cenozoic Globigerinidae. In: A study of the morphology, taxonomy, evolutionary relationships and the stratigraphical distribution of some Globigerinidae (mainly Globigerinacea), vol 3. Brill, Leiden, The Netherlands, pp 1–1413

Bolle MP, Adatte T, Keller G, Von Salis K, Hunziker J (1998) Stratigraphy, mineralogy and geochemistry of the Trabakua Pass and Ermua sections in Spain: Paleocene–Eocene transition. Eclogae Geol Helv 91:1–25

Bolle MP, Adatte T, Keller G, Salis K von, Burns S (1999) The Paleocene-Eocene transition in the Southern Tethys (Tunisia): climatic and environmental fluctuations. Bull Soc Géol France 170:661–680

Boon JJ, Rijpstra WIC, Lange F de, Leeuw JW de, Yoshioka M, Shimizu Y (1979) The Black Sea sterol: a molecular fossil for dinoflagellate blooms. Nature 277:125–127

Bralower TJ, Zachos JC, Thomas E, Parrow M, Paul CK, Kelly DC, Premoli Silva I, Sliter WV, Lohmann KC (1995) Late Paleocene to Eocene paleoceanography of the equatorial Pacific Ocean: stable isotopes recorded at Ocean Drilling Program Site 865, Allison Guyot. Paleoceanography 10:841–865

Calvert SE (1987) Oceanographic controls on the accumulation of organic matter in marine sediments. In: Brooks J, Fleets AJ (eds) Marine petroleum source rocks. Geol Soc Lond Spec Publ 26:137–151

Cande SC, Kent DV (1992) A new geomagnetic polarity time scale for the Late Cretaceous and Cenozoic. J Geophys Res 97:13917–13951

Chamley H (1989) Clay sedimentology. Springer, Berlin Heidelberg New York, pp 1–623

Chamley H (1998) Clay mineral sedimentation in the ocean. In: Paquet H, Clauer N (eds) Soils and sediments, mineralogy and geochemistry. Springer, Berlin Heidelberg New York, pp 269–302

Corfield RM, Cartlidge JE, Premoli-Silva I, Housley RA (1991) Oxygen and carbon isotope stratigraphy of the Palaeogene and Cretaceous limestones in the Bottacione Gorge and the Contessa Highway sections, Umbria, Italy. Terra Nova 3:414–422

Dickens GR, O'Neil JR, Rea DK, Owen RM (1995) Dissociation of oceanic methane hydrate as a cause of the carbon isotope excursion at the end of the Palaeocene. Nature 353:319–322

Dickens GR, Castillo M, Walker JC (1997) A blast of gas in the latest Paleocene: simulating first-order effects of massive dissociations of oceanic methane hydrate. Geology 25:259–262

Espitalié J, Deroo G, Marquis F (1985) La pyrolyse Rock-Eval et ses applications. Parts 1 and 2. Rev Inst France Pétrogr 40:5–6

Espitalié J, Deroo G, Marquis (1986) La pyrolyse Rock-Eval et ses applications. Part 3. Rev Inst France Pétrogr 41:1

Estes R, Hutchison JH (1980) Eocene lower vertebrates from Ellesmere Island, Canadian Arctic Archipelago. Palaeogeogr Palaeoclimatol Palaeoecol 30:325–347

Freeman KH, Hayes JM, Trendel J-M, Albrecht P (1990) Evidence from carbon isotope measurements for diverse origins of sedimentary hydrocarbons. Nature 343 : 254–256

Gagosian RB, Smith SO (1979) Steroids ketones in surface sediments from the south-west African shelf. Nature 277 : 287–289

Gavrilov YO, Muzylev NG (1991) The geochemistry of sapropelic interbeds in the Paleogene of the central Caucasus. Lithol Mineral Resourc 26 : 485–590

Gavrilov YO, Kodina LA, Lubchenko IY, Muzylev NG (1997) The Late Paleocene anoxic event in epicontinental seas of Peri-Tethys and formation of the Sapropelite Unit: sedimentology and geochemistry. Lithol Mineral Resourc 32 : 427–450

Gawenda P, Winkler W, Schmitz B, Adatte T (1999) Climate and bioproductivity control on carbonate turbidite sedimentation (Paleocene to earliest Eocene Gulf of Biscay, Zumaia). J Sediment Res 69 : 1253–1261

Gibbs RJ (1977) Clay mineral segregation in the marine environment. J Sediment Petrol 47 : 237–243

Gibson TG, Bybell LM, Owens JP (1993) Latest Paleocene lithologic and biotic events in neritic deposits of southwestern New Jersey. Paleoceanography 8 : 495–514

Gingerich PD (1980) Evolutionary patterns in Early Cenozoic mammals. Ann Rev Earth Planet Sci 8 : 407–424

Hallam A, Bradshaw MJ (1979) Bituminous shales and oolitic ironstones as indicators of transgressions and regressions. J Geol Soc Lond 136 : 157–164

Haq BU, Hardenbol J, Vail PR (1988) Mesozoic and Cenozoic chronostratigraphy and cycles of relative sea level change. In: Wilgus CK et al. (eds) Sea level changes: an integrated approach. SEPM Spec Publ 42 : 71–108

Hayes JM (1993) Factors controlling $\delta^{13}C$ contents of sedimentary organic compounds: principles and evidence. Mar Geol 113 : 111–125

Hayes JM, Popp BN, Takigiku R, Johnson MW (1989) An isotopic study of biogeochemical relationships between carbonates and organic carbon in the Greenhorn Formation. Geochim Cosmochim Acta 53 : 2961–2972

Hinrichs K-U, Hayes JM, Sylva SP, Brewer PG, DeLong EF (1999a) Methane-consuming archaebacteria in marine sediments. Nature 398 : 802–805

Hinrichs K-U, Schneider RR, Müller PJ, Rullkötter J (1999b) A biomarker perspective on paleoproductivity variations in two Late Quaternary sediment sections from the Southeast Atlantic Ocean. Org Geochem 30 : 341–366

Hinrichs K-U, Summons RE, Orphan V, Sylva SP, Hayes JM (1999) Molecular and isotopic analyses of anaerobic methan oxidizing communities in marine sediments. Org Geochem 32

Ilyin AV, Boiko VS (1989) The Kisil Kum phosphorite deposits, Middle Asia, USSR. In: Notholt A et al. (eds) Phosphate deposits of the world. Cambridge University Press, Cambridge, pp 507–509

Kaiho K, Arinobu T, Ishiwatari R, Morgans HEG, Okada H, Takeda N, Tazaki K, Zhou G, Kajiwara Y, Matsumoto R, Hirai A, Niitsuma N, Wada H (1996) Latest Paleocene benthic foraminiferal extinction and environmental changes at Tawanui, New Zealand. Paleoceanography 11 : 447–465

Kazmin VG, Sbortshikov IM, Ricou LE, Zonenshain LP, Boulin J, Knipper AL (1986) Volcanic belts as markers of the Mesozoic–Cenozoic active margin of Eurasia. Tectonophysics 123 : 123–152

Kelly DC, Bralower TJ, Zachos JC, Premoli Silva I, Thomas E (1996) Rapid diversification of planktonic foraminifera in the tropical Pacific (ODP Site 865) during the Late Paleocene Thermal Maximum. Geology 24 : 423–426

Kennett JP, Stott L (1990) Proteus and Proto-Oceanus: Paleogene oceans as revealed from Antarctica stable isotopic results. Proc ODP Sci Results 113 : 865–879

Kennett JP, Stott L (1991) Abrupt deep-sea warming, palaeoceanographic changes and benthic extinctions at the end of the Paleocene. Nature 353 : 225–229

Knox RW (1996) Correlation of the early Paleogene in northwest Europe: an overview. In: Knox R et al. (eds) Correlation of the Early Paleogene in Northwest Europe. Geol Soc Lond Spec Publ 101 : 1–11

Kübler B (1983) Dosage quantitatif des minéraux majeurs des roches sédimentaires par diffraction X. Cahiers Inst Géol Neuch Suisse Série AX 1.1 and 1.2

Kübler B (1987) Cristallinité de l'illite, méthodes normalisées de préparations, méthodes normalisées de mesures. Cahiers Inst Géol Neuch Suisse Série ADX

Kusnetsova NV (1952) New data on stratigraphy of the Later Tertiary deposits of Mangyshlak. Dokl AN USSR nov ser 82 : 143–146

Lafargue E, Espitalié J, Marquis F, Pillot D (1996) Rock Eval 6 applications in hydrocarbon exploration, production and in soil contamination studies. Rock Eval user manual. Vinci Technologies, Rueil Malmaison, France, pp 1–37

Lu G, Keller G (1993) The Paleocene–Eocene transition in the Antarctic Indian Ocean: inference from planktic foraminifera. Mar Micropaleontol 21 : 101–142

Lu G, Keller G (1995) Planktic foraminiferal faunal turnovers in the subtropical Pacific during the Late Paleocene to Early Eocene. J Foram Res 25 : 97–116

Lu G, Keller G, Adatte T, Benjamini C (1995) Abrupt change in the upwelling system along the southern margin of the Tethys during the Paleocene–Eocene transition event. Israel J Earth Sci 44 : 185–195

Lu G, Keller G, Adatte T, Ortiz N, Molina E (1996) Long-term (10^5) or short-term (10^3) $\delta^{13}C$ excursion near the Palaeocene–Eocene transition : evidence from the Tethys. Terra Nova 8 : 347–355

Lu G, Adatte T, Keller G, Ortiz N (1998a) Abrupt climatic, oceanographic and ecologic changes near the Paleocene–Eocene transition in the deep Tethys basin: the Alamedilla section, southern Spain. Eclogae Geol Helv 91 : 293–306

Lu G, Keller G, Pardo A (1998b) Stability and change in Tethyan planktic foraminifera across the Paleocene–Eocene transition. Mar Micropaleontol 35 : 203–233

Martini E (1971) Standard Tertiary and Quaternary calcareous nannoplankton zonation. In: Farinacci A (ed) Proc 2nd Planktonic Conference, Roma, pp 739–785

Mélières F (1977) X-ray mineralogy studies, Leg 41 DSDP, eastern North Atlantic Ocean. Init Rep Deep Sea Drilling Project 41 : 1065–1086

Millot G (1970) Geology of clays. Springer, Berlin Heidelberg New York, pp 1–425

Moore D, Reynolds R (1989) X-Ray diffraction and the identification and analysis of clay minerals. Oxford University Press, Oxford, pp 1–332

Muzylev NG, Nishankhodzhaev RN, Rasulov UM, Salibaev GK, Ibragimov RN (1994) Upper Paleocene oil shales in Central Asia. Litol Polezn Iskop 1 : 131–135 [in Russian]

Muzylev NG, Beníyamovskii VN, Gavrilov YO, Shcherbinina EA, Stupin SI (1996) Paleontological and geochemical features of the Lower Paleocene Saproprel in the Central Ciscaucasus. In: Kuznetsova KI, Muzylev NG (eds) Fossil microorganisms as the basis of stratigraphy, correlation, and paleogeography of the Phanerozoic. GEOS, Moscow, pp 117–126 [in Russian]

Oberhänsli H (1992) The influence of the Tethys on the bottom waters of the Early Tertiary ocean. In: Kennett JP (ed) The Antarctic paleoenvironment: a perspective on global change. Antarctic Research Service, pp 167–184

Oberhänsli H, Keller G, Adatte T, Pardo A (1998) Diagenetically and environmentally controlled changes across the K/T transition at Koshak, Mangyshlak (Kazakhstan). Bull Soc Géol France 169 : 493–501

O'Connell SBO (1990) Variations in Upper Cretaceous and Cenozoic calcium carbonate percentages, Maud Rise, Weddell Sea. Proc ODP Sci Results 113 : 971–984

Pardo A, Keller G, Oberhänsli H (1999a) Paleoecologic and paleoceanographic evolution of the Tethyan realm during the Paleocene–Eocene transition. J Foram Res 29 : 37–57

Pardo A, Bolle MP, Keller G (1999b) El evento bio-climatico del transito P–E en el Paratethys boreal: datas de $\delta^{13}C$, $\delta^{18}O$ y foraminiferos planctonicos. Rev Esp Micropaleontol 31 : 91–96

Perch-Nielsen K (1985) Cenozoic calcareous nannofossils. In: Bolli HM, Saunders JB, Perch-Nielsen K (eds) Plankton stratigraphy. Cambridge University Press, Cambridge, pp 427–454

Premoli-Silva I, Boersma A (1984) Atlantic Eocene planktonic foraminiferal historical biogeographic and paleohydrologic indices. Palaeogeogr Palaeoclimatol Palaeoecol 67 : 315–356

Reeburgh WS (1976) Methane consumption in Cariaco trench waters. Earth Planet Sci Lett 28 : 337–344

Robert C (1982) Modalité de la sédimentation argileuse en relation avec l'histoire géologique de l'Atlantique Sud. PhD thesis, Univ Aix-Marseille II, France, pp 1–141

Robert C, Chamley H (1991) Development of early Eocene warm climates, as inferred from clay mineral variations in oceanic sediments. Palaeogeogr Palaeoclimatol Palaeoecol 89 : 315–332

Robert C, Kennett JP (1992) Paleocene and Eocene kaolinite distribution in the South Atlantic and Southern Ocean: Antarctic climatic and paleoceanographic implications. Mar Geol 103 : 99–110

Robert C, Kennett JP (1994) Antarctic subtropical humid episode at the Paleocene–Eocene boundary: clay-mineral evidence. Geology 22 : 211–214

Robinson N, Eglinton G, Brassell SC, Cranwell PA (1984) Dinoflagellate origin of sedimentary 4α-methylsteroids and 5α (H)-stanols. Nature 308 : 439–442

Rohmer M, Bouvier-Nave P, Ourisson G (1984) Distribution of hopanoid triterpenes in prokaryotes. J General Microbiol 130 : 1137–1150

Schneider S, Schneider R (1990) Verteilung der Moore auf der Erde. In: Göttlich K (ed) Moor- und Torf- Kunde. E.Schweizerbart'sche Verlagsbuchhandlung. Nägele and Obermiller, Stuttgart, Germany, pp 65–101

Sloan LC, Walker JCG, Moore TC Jr, Rea DK, Zachos JC (1992) Possible methane-induced polar warming in the early Eocene. Nature 357 : 320–322

Summons RE, Jahnke LJ, Roksandic Z (1994) Carbon isotopic fractionation in lipids from methanotrophic bacteria: relevance for interpretation of the geochemical record of biomarkers. Geochim Cosmochim Acta 58 : 2853–2863

Smith A, Smith D, Funnell B (1994) Atlas of Mesozoic and Cenozoic Coastlines. Cambridge University Press, Cambridge, pp 1–99

Tissot BP, Welte DH (1984) Petroleum formation and occurrence. Springer, Berlin Heidelberg New York, pp 1–699

Thomas E (1990) Late Cretaceous through Neogene deep-sea benthic foraminifers (Maud Rise, Weddell Sea, Antarctica). Proc ODP Sci Results 113 : 571–594

Thomas E, Shackleton NJ (1996) The Paleocene–Eocene benthic foraminiferal extinction and stable isotope anomalies. In: Knox RO et al. (eds) Correlations of the early Paleogene in Northwest Europe. Geol Soc Lond Spec Publ 101 : 401–411

Toumarkine M, Luterbacher P (1985) Paleocene and Eocene planktic foraminifera. In: Bolli et al. (eds) Plankton stratigraphy. Cambridge University Press, Cambridge, pp 87–154

Volkman JK, Kearney P, Jeffrey SW (1990) A new source of 4-methyl sterols and 5α(H)-stanols in sediments: prymnesiophyte microalgae of the genus *Pavlova*. Org Geochem 15 : 489–497

Volkman JK, Barret SM, Dunstan GA, Jeffrey SW (1993) Geochemical significance of the occurrence of dinosterol and other 4-methyl sterols in a marine diatom. Org Geochem 20 : 7–16

Wakeham SG (1990) Algal and bacterial hydrocarbons in particulate matter and interfacial sediment of the Cariaco Trench. Geochim Cosmochim Acta 54 : 1325–1336

Wetzel A (1991) Stratification in black shales: depositional models and timing: an overview. In: Einsele et al. (eds) Cycles and events in stratigraphy. Springer, Berlin Heidelberg New York, pp 508–523

Wolfe JA (1980) Tertiary climates and floristic relationships at high latitudes in the northern hemisphere. Palaeogeogr Palaeoclimatol Palaeoecol 30 : 313–323

Zachos JC, Lohmann KC, Walker JCG, Wise SW (1993) Abrupt climate change and transient climates during the Paleogene: a marine perspective. J Geology 101 : 191–213